Atomic Spectroscopy

July/August 2003   Volume 24, No. 4

In This Issue:

**Issues also
available
electronically.**

(see inside front cover)

PerkinElmer®
precisely.

Determination of Selenium in Animal Feed by Hydride Generation AAS: Validation of Analytical Method

*Cathal D. Connolly[a], Ronan F. Power[a], and Michael J. Hynes[b]

[a] Alltech Biotechnology Centre, Summerhill Road, Dunboyne, Co. Meath, Ireland
[b] Department of Chemistry, National University of Ireland, Galway, Ireland

INTRODUCTION

Selenium is an essential nutrient in the diets of animals, with deficiencies causing problems such as white muscle disease in calves and lambs, exudative diathesis in poultry, and hepatosis in pigs (1). Several studies have revealed the importance of selenium in human nutrition and maintaining an adequate Se status has been linked to decreased incidences of cancer, heart disease, and arthritis (2). Selenium-containing enzymes such as glutathione peroxidases together with vitamin E protect cells from oxidative damage and slow down the process of cell aging (3). Selenium enters the food chain when it is taken up from the soil and incorporated into plant protein. The level of plant Se depends greatly on the concentration of selenium in the soil, plant type, and growth conditions. Soil selenium concentrations are typically in the range 0.1–2.0 mg/kg, but due to uneven distribution can vary from 0–100 mg/kg with deficiency being a more common problem than overabundance (4). It has therefore become customary to supplement animal and human diets with sources of selenium in an effort to control intake and prevent the problems associated with Se deficiency. Schrauzer (5) recommends that the supplemented selenium should be in its natural form, L-selenomethionine (SeMet) which can either be prepared synthetically or supplied as selenium-enriched yeast. While Se supplementation may be necessary to avoid deficiency, adding too much selenium to the diet can also cause problems. Therefore, accurate

*Corresponding author.
e-mail: cconnolly@alltech.com

ABSTRACT

A procedure using open digestion followed by hydride generation atomic absorption spectrometry is described for measuring the selenium content of cereal-based animal feed. Accurate and precise data can be obtained after careful preparation of the samples prior to analysis. The limits of detection and quantitation were 1 ng and 2.5 ng Se, respectively. The signal response was linear over the range of 2.5 to 250 ng Se, and the average recovery from the spiked samples was 102.5%. The validated method was used to measure the Se content of wheat flour standard reference material resulting in 1.21 ± 0.035 mg/kg (n = 3) which is in good agreement with the certified level of 1.23 ± 0.09 mg/kg.

quantitation of selenium levels in feed is important and methods have been published that describe sample preparation and the determination of selenium in various samples (6–9). Some of the techniques used are very sophisticated and beyond the reach of many laboratories; thus there is a need for simple but reliable ways to quantify Se in animal feed. It is also important to properly evaluate the procedures used to obtain samples for analysis because there is a potential for error in the sampling of particulate mixtures such as feed (10).

The aim of the present work was to validate a method for the determination of Se in feed with a high degree of accuracy and precision using hydride generation atomic absorption spectrometry (HGAAS). Other validation parameters were also investigated in accordance with approved guidelines (11–13)

to assess the overall suitability of the method.

EXPERIMENTAL

Instrumentation

A PerkinElmer AAnalyst™ 100 atomic absorption spectrometer (PerkinElmer Life and Analytical Sciences, Shelton, CT, USA) was used, equipped with deuterium background corrector and MHS-10 hydride generator. The selenium electrodeless discharge lamp was operated at 200 mA at a wavelength of 196.0 nm and a spectral bandwidth of 2.0 nm. The quartz tube was heated in a lean blue oxidizing flame of air:acetylene (3:1), and nitrogen was used as the carrier gas.

Reagents

Analytical grade concentrated acids (70% HNO_3, 70% $HClO_4$, 37% HCl) were supplied by Fisher Scientific (UK). Selenium calibration standards were prepared daily from a 1000-µg/mL solution (Aldrich Chemical Co.) in HCl (10% v/v) with deionized water. The reductant reagent for hydride generation, 3% (w/v) $NaBH_4$ in 1% (w/v) NaOH, was also prepared fresh daily.

Test Samples

Animal Feed

Samples were taken from a commercially prepared cereal-based poultry feed ration, formulated to contain 0.28 mg/kg Se as Selplex™ (selenium yeast containing 2000 mg/kg Se, from Alltech Inc., KY, USA). A 1-kg composite sample of feed was mechanically ground to a uniform particle size (< 1 mm) and mixed for 20 minutes in a double-cone blender at 8 rpm to ensure sample homogeneity before taking sub-samples for analysis. It is very

important to prepare the feed sample carefully to avoid highly variable results.

Standard Reference Material

Wheat Flour SRM 8436 (certified Se content = 1.23 ± 0.09 mg/kg) was obtained from the National Institute of Standards and Technology, Gaithersburg, MD, USA.

Digestion

Samples of feed (2.0 g) and Wheat Flour SRM 8436 (1.0 g) were placed in 200x42-mm Pyrex® digestion tubes. Concentrated HNO_3 (10 mL) was added and the mixture heated at 110ºC using an Electrothermal (Electrothermal Engineering Ltd., Essex, UK) heating mantle until the foaming subsided. Concentrated $HClO_4$ (5 mL) was added and heating at 110ºC continued until the evolution of dense brown fumes had stopped. The temperature was then increased to 250ºC and the digestion process monitored closely as prolonged boiling or overheating of the digests may result in loss of volatile Se compounds. Digestion was complete when the dense white fumes of $HClO_4$ began to reflux in the upper neck of the tube and the solution stopped effervescing and boiled gently. Digested samples were cooled to room temperature before adding 10 mL of concentrated HCl and boiling for 10 minutes. This step was necessary to convert any Se(VI) formed during digestion to Se(IV) for hydride generation. Finally, the reduced digests were cooled to room temperature and diluted to 50 mL using deionized water.

Instrument Calibration

A calibration curve (20–100 ng Se) was constructed after zeroing the instrument using 10 mL of 45% (v/v) HCl. Aliquots of 20 μL, 50 μL, and 100 μL of a 1-mg/L selenium stock solution were added to 10 mL of 45% HCl to correspond to 20 ng, 50 ng, and 100 ng Se, respectively. Each standard was analyzed in triplicate.

Sample Analysis

Aliquots of feed digest (2 mL) were added to 10 mL of 45% HCl in the reaction flask. For Wheat Flour SRM 8436, 1-mL aliquots were used because of the higher concentration of selenium. All samples were analyzed in triplicate.

Statistical Analysis

Experimental data were analyzed using Minitab (Minitab Inc., Coventry, UK) and a linear least squares program (LESQ) based on the equations provided in Reference (14). Method performance and acceptance criteria were set using the Horwitz function in accordance with the guidelines in Reference (11).

RESULTS AND DISCUSSION

Precision and Repeatability

Precision is a measure of agreement between observed values obtained by repeated application of the same analytical procedure to the same homogeneous sample under documented conditions. The results from the analysis of 10 separate samples of poultry feed are presented in Table I.

Repeatability is an expression of assay precision under the same operating conditions over a short interval of time. It is a measure of the expected difference between the results obtained by repeated application of the analytical procedure to an identical test sample under identical conditions. This was determined by recording 10 readings of a single feed sample digest (see Table II).

Limits of Detection and Quantitation

The observed relative standard deviation (RSD) for each set of data

TABLE I
Method Precision

Sample No.	Se (mg/kg)
1	0.276
2	0.249
3	0.272
4	0.300
5	0.254
6	0.266
7	0.274
8	0.315
9	0.255
10	0.277

Mean ± SEM = 0.274 ± 0.006 mg/kg.

TABLE II
Method Repeatability

Replicate No.	Se (mg/kg)
1	0.241
2	0.267
3	0.283
4	0.251
5	0.282
6	0.261
7	0.266
8	0.261
9	0.295
10	0.293

Mean ± SEM = 0.270 ± 0.006 mg/kg.

was compared to the value calculated using the Horwitz function. Adequate precision was indicated when the observed RSD was less than or equal to the calculated RSD.

A visual evaluation approach was used to establish the limit of detection (LOD) of the method. Five replicates of standard solutions of decreasing Se concentration were analyzed until the signal disappeared or was too small to be reliably detected. The results are shown in Table III. The limit of detection is the lowest amount of analyte in a sample that can be detected but not necessarily quantitated as an exact value. This was

found to be 1 ng Se because the signal produced at this level could not be accurately and precisely (RSD ≤ 16%) measured.

The limit of quantitation (LOQ) is defined as the minimum level at which the analyte may be quantified with acceptable accuracy and precision. A visual evaluation approach was used to determine this level by analyzing samples containing known concentrations of analyte.

The minimum amount of Se that could be accurately and precisely (RSD ≤ 16%) measured was found to be 2.5 ng (Table III).

TABLE III
Limit of Detection/Quantitation

Se (ng)	Measured Se (ng)[a]
5.0	5.34 ± 0.12
2.5	2.48 ± 0.11
1.0	0.55 ± 0.25

[a] Mean ± SEM; n = 5.

Linearity and Range

The linearity of an analytical procedure is its ability (within a given range) to obtain test results that are directly proportional to the amount of analyte in the sample. A linear range for the method was determined by replicate analysis of samples containing amounts of analyte at the limit of quantitation and at levels of 5, 10, and 100 times the LOQ. The results are presented in Table IV. Analysis of these data using the LESQ statistics computer program revealed a correlation coefficient of 0.99970 and demonstrated good linearity of the method over the range of 2.5 to 250 ng Se.

TABLE IV. Linearity/Range

Se (ng)	Measured Se (ng)[a]
2.5	2.48 ± 0.11
12.5	12.82 ± 0.50
25	23.44 ± 0.98
250	258 ± 8

[a] Mean ± SEM; n = 5.

Specificity and Selectivity

The terms specificity and selectivity relate to the method's ability to distinguish between the analyte and other components in the test sample. This discriminating power may be determined by spiking test samples with a known amount of analyte and measuring its recovery in the presence of the sample matrix. Selenium was added to five replicate samples at a rate corresponding to 0.15 and 0.30 mg/kg in the feed and the recovery data are presented in Table V.

TABLE V. Specificity/Selectivity

Se Spike (mg/kg)	Recovery (%)[a]
0.15	103.9 ± 2.3
0.30	101.1 ± 0.9

[a] Mean ± SEM; n = 5.

Accuracy

Defined as the closeness in agreement between the experimental value and an accepted reference value, accuracy may be inferred once specificity, linearity, and precision have been established. It is also customary to assess method accuracy by applying the analytical procedure to a standard reference material that contains a certified concentration of analyte. The results for the analysis of Wheat Flour SRM 8436 are shown in Table VI.

CONCLUSION

The analytical method described is suitable for accurate and precise determination of selenium at levels typically found in commercially prepared cereal-based animal feed.

TABLE VI. SRM Analysis (Method Accuracy)

Sample	Measured Se (mg/kg)[a]	Certified Se (mg/kg)
Wheat Flour SRM 8436	1.21 ± 0.035	1.23 ± 0.09

[a] Mean ± SEM; n = 3.

REFERENCES

1. K.A. Jacques, Feed Compounder (January: 14, 2002).
2. M.P. Rayman, Lancet 356, 233 (2000).
3. S.E. Raptis, G. Kaiser, and G. Tolg, Fresenius' J. Anal. Chem. 316, 105 (1983).
4. J.E. Oldfield, Selenium World Atlas, Selenium-Tellurium Development Association, Grimbergen, Belgium (1999).
5. G.N. Schrauzer, Nutrition 130, 1653 (2000).
6. B. Welz and M. Melcher, Anal. Chim. Acta 165, 131 (1984).
7. J. Neve, M. Hanocq, and L. Molle, Mikrochim. Acta 1, 259 (1980).
8. P. Hocquellet and M.-P. Candillier, Analyst 116, 505 (1991).
9. M. Verlinden, H. Deelstra, and E. Adriaenssens, Talanta 28, 637 (1981).
10. B. Kratochvil, S.R. Reid, and W.E. Harris, Chem. Ed. 57, 7: 518 (1980).
11. C. Burgess, Valid analytical methods and procedures, Royal Society of Chemistry, Cambridge, UK. (2000).
12. European Agency for the Evaluation of Medicinal Products, CPMP/ICH/381/95 (1995).
13. European Agency for the Evaluation of Medicinal Products, CPMP/ICH/281/95 (1996).
14. J.C. Miller and J.N. Miller, Statistics for analytical chemistry, 2nd ed., Ellis Horwood Ltd., Chichester, UK (1988).

On-line Solid Phase Extraction Preconcentration of Ultratrace Amounts of Zinc in Fractionated Soil Samples for Determination by Flow Injection Flame AAS

C.R. Preetha, V.M. Biju, and *T. Prasada Rao
Ultra Trace Analysis Group, Regional Research Laboratory (CSIR)
Trivandrum - 695 019, India

INTRODUCTION

Solid phase extraction (SPE) is currently being used as a separation/preconcentration procedure whenever complex matrices have to be analyzed or low concentrations of analytes have to be determined. SPE has become the method of choice in many laboratories for the analysis of complex samples due to its ease of automation, low reagent consumption, absence of emulsion formation, flexibility, and for providing higher enrichment factors (1–2). Further, SPE is environmentally friendlier than liquid-liquid extraction since it requires lower volumes of solvents (2–4). Flow injection (FI) on-line SPE preconcentration and matrix separation is a powerful technique which effectively enhances the selectivity, sensitivity, and precision of flame AAS (FAAS) (5,6).

Zinc is an important requirement for the satisfactory growth of plants. It is a micro nutrient and activates enzymes in plants. Zinc is involved in protein synthesis and is essential for the maintenance of auxin, a growth substance. Zinc deficiency results in various growth abnormalities such as chlorosis and interveinal yellowing on young leaves, reducing leaf size and causes shortening of the internodes. Excess zinc may also cause iron deficiency in some plants (7). Hence, the routine monitoring of zinc in soils, which can contain from 1–80 mg/kg, is important (8).

The determination of distinct chemical species, often referred to

*Corresponding author.
e-mail: tprasadarao@rediffmail.com
Fax: 0471-491712

ABSTRACT

A flow injection on-line solid phase extraction (SPE) preconcentration system coupled to a flame atomic absorption spectrometer (FAAS) was developed for the determination of zinc at the µg L^{-1} level. Zinc is complexed with 1-(2-thiazoly-lazo)-2-naphthol (TAN) in the pH range of 9.5–11.0 in the flow injection system and adsorbed onto a C$_{18}$-bonded silica gel micro column. The preconcentrated Zn-TAN complex was eluted with acidified methanol (pH~2). The eluent was injected directly into the nebulizer of a FAAS for measurement. The enrichment factor was 120 with a 1-min preconcentration time and a sample throughput of 30 h^{-1}. The detection limit corresponding to three times the standard deviation of the blank was 0.15 µg L^{-1} with a precision of 2.5% (RSD) for five successive determinations of 5 µg L^{-1} of Zn. No significant interference was observed from neutral electrolytes and cations of soil samples. The method was also applied successfully in the analysis of soils which were fractionated as per BCR (now Standards, Measurements and Testing Program) using both the direct and standard addition (SA) methods.

as speciation, is widely acknowledged to be of vital importance in environmental analysis. While it is often possible to define a particular compound or oxidation state when dealing with solutions, it is far more difficult to characterize the actual form of an element in solids such as soils (9). Pickering (10) has summarized a series of reagents used for fractionation of soil samples ranging from water to concentrated acids.

In 1987, the Bureau of Community Reference (BCR) consisting of various European experts have started a program to harmonize the methodology. In 1994, the BCR reported a sequential fractionation scheme adopted in different stages (11,12).

Various FIA procedures developed for zinc are summarized in Table I. Recently we have described an on-line SPE preconcentration flame AAS determination of copper in seawater samples (22). This paper describes for the first time an on-line solid phase preconcentration with TAN as the chelating agent and its subsequent sorption onto a C$_{18}$ bonded silica gel, followed by elution with methanol. The FIAS-FAAS procedure thus developed allows the determination of zinc down to 2 ng g^{-1} of soil.

EXPERIMENTAL

Instrumentation

A PerkinElmer Model AAnalyst™ 100 atomic adsorption spectrometer (PerkinElmer Life and Analytical Sciences, Shelton, CT, USA) with deuterium background correction and a PerkinElmer Lumina® hollow cathode lamp were used. The hollow cathode lamp current, wavelength, and spectral bandpass were 30 mA, 213.9 nm, and 0.7 nm, respectively. A standard air-acetylene stainless steel nebulizer and a 10-cm path length system was operated at an airflow rate of 4.0 L/min and an acetylene flow rate of 1.0 L/min. The burner height was adjusted to about 30 mm from base for optimum sensitivity. The nebulizer uptake rate was adjusted to provide optimum response for conventional sample aspiration.

A PerkinElmer FIAS™-400 flow injection system, connected to the spectrometer, was used for the on-line preconcentration of zinc. The automatic operation of the injection valve and two multichannel peristaltic pumps were programmed using the spectrometer software (PerkinElmer AA WinLab™ V. 3.0). Tygon® peristaltic pump tubing was used to pump the sample (7.0 mL/min) and reagents (3.0 mL/min); PTFE tubing of 0.3 mm i.d was used for all connections in order to minimize dead volume. A commercially available conical-shaped micro column of 50-μL capacity (PerkinElmer) packed with 20 mg of C_{18} bonded silica gel (40–60 μM) was used. Time-resolved absorbance signals of zinc were displayed on the computer monitor along with peak height and integrated absorbance values.

Reagents and Standard Solutions

All reagents used were of analytical reagent grade. 1-(2-thiazolylazo)-2-naphthol (TAN) 0.005% (Aldrich, Milwaukee, WI , USA) was prepared in 0.5 M ammonia solution as it is not soluble in pure water. Methanol acidified to pH~2 with HNO_3 was used for elution of the zinc adsorbed on the micro column. 0.1 M (pH 10) NH_3-NH_4Cl buffer was used for the pH adjustments.

Stock standard solution of 1 mg mL⁻¹ of zinc was prepared by dissolving 1.0973 g of zinc sulfate hepta hydrate (Aldrich, USA) in 250 mL of deionized water. This solution was standardized by using the EDTA titration procedure. The working solutions were prepared by suitable dilution.

Procedure

The FI manifold (0.3 mm i.d) used for the on-line preconcentration and elution was described by Sperling et al. (23). The samples and ammoniacal TAN solutions were pumped simultaneously and

mixed on-line. Preconcentration time was approximately 60 s and the sorbed zinc was eluted at a rate of 4 mL/min with methanol acidified to pH ~2. A linear calibration curve was obtained for 0–50 μg L⁻¹ of zinc using aqueous standard solutions in the sample stream.

Analysis of Soil Samples

Fractionation Procedure

The soil samples were collected at 12 different locations, then dried and ground to a fine powder in an agate mortar and pestle. Sufficient care was taken to avoid cross-contamination during grinding by thorough washing. Figure 1 is a schematic diagram which shows the sequential extraction procedure used to determine extractable trace metals in soils.

About 1 g of soil sample was weighed and then stirred for 24 h in a 100-mL beaker with 40 mL of 0.1 M of CH_3COOH.

The filtrate (Fraction I) was collected and saved for subsequent analysis. The residue was transferred into a 100-mL beaker, stirred for 24 h with 40 mL of

0.10M NH_2OH•HCl, and the pH adjusted to 2–3 with HNO_3.

The filtrate (Fraction II) was collected and saved for subsequent analysis. The residue was transferred to a 100-mL beaker, treated with 2 x 10 mL of 8.8M H_2O_2 (with the pH adjusted to 2–3), and evaporated to near dryness in each case. Subsequently, 50 mL of 1M NH_4OAc (pH ~2) was added and stirred for 24 h.

The filtrate (Fraction III) was collected and saved for subsequent analysis. The residue from Fraction III was mineralized in a platinum crucible after addition of 10 mL each of HNO_3 and HF.

After complete dissolution and evaporation of the HF, the resulting solution was diluted to 50 mL with deionized water. This solution (Fraction IV) was saved for subsequent analysis.

The four fractions collected for each sample were adjusted to pH ~10 using concentrated NH_3 prior to on-line SPE preconcentration and flame AAS determination.

TABLE I
Summary of FIA Procedures Developed Since 1990
for the Determination of Zinc

Sample No.	Detection technique	Detection limit (ng mL⁻¹)	Linear range (μg mL⁻¹)	Sampling frequency	Application	Reference
1.	UV Visible-	–	–	–	–	13
2.	Fluorescence	3		–	–	14
3.	Flame AAS	–	–	40	–	15
4.	Flame AAS	100	0.1–0.5	–	–	16
5.	Flame AAS	1	–	–	–	17
6.	Flame AAS	–	–	–	–	18
7.	Flame AAS	0.5	0.0005–0.05	30	Marine sediment and sea plant	19
8.	ICP-AES	–	–	–	–	20
9.	ICP-AES	3.6	0.01–20	-	-	21
10.	Flame AAS	0.15	0.0005–0.05	30	Soil samples	Present method

Sample
(1 g)

0.10 M of CH$_3$COOH, 40 mL g^{-1} (v/m)
30^{0}C Stir for 24 h on magnetic stirrer

Solution → Fraction I

Residue

0.10 M NH$_2$OH. HCl, (pH 2-3 with HNO$_3$) 40 mL g^{-1} (v/m)
30^{0}C, Stir for 24 h on magnetic stirrer

Solution → Fraction II

Residue

8.8 M H$_2$O$_2$ (pH 2-3 with HNO$_3$), 10 mL g^{-1} (v/m)
Room temperature 1h, 85^{0}C 1h, reduce volume to few mL. Repeat above process once again. 1M NH$_4$O
Ac (pH 2 with HNO$_3$), 50 mL g^{-1} (v/m) 30^{0}C Stir for 24 h on magnetic stirrer

Solution → Fraction III

Residue

HNO$_3$ – HF Digestion, Expel HF, Make up to 50 mL with deionized water
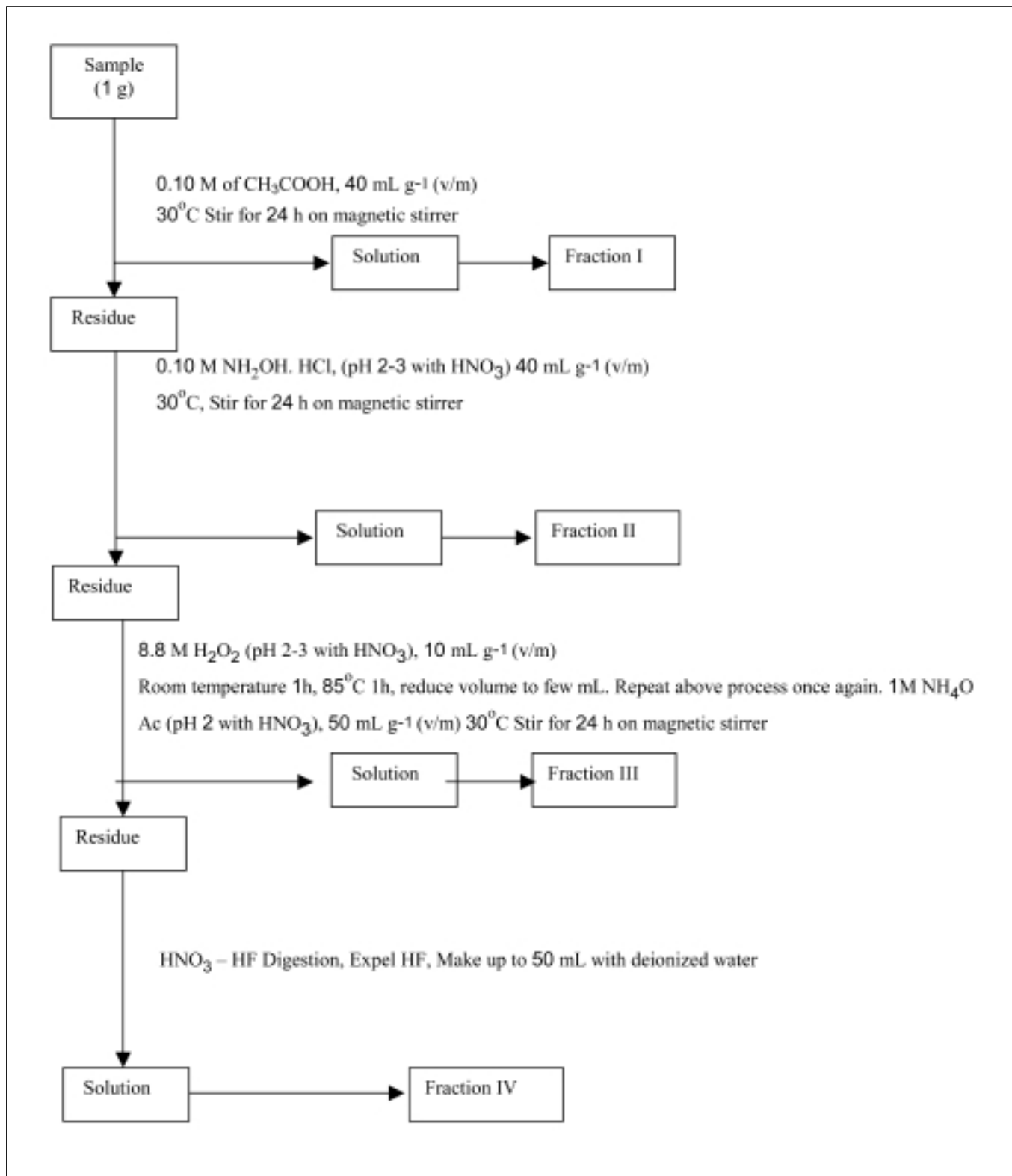
Solution → Fraction IV

Fig. 1. Schematic of the sequential extraction procedure to determine extractable trace metals in soils.

RESULTS AND DISCUSSION

Background correction was necessary since separation by sorption did not eliminate concomitant species which caused non-specific absorption. A detailed evaluation and the optimization of various analytical parameters during the FIAS-FAAS determination of zinc are given below.

Optimization of Analytical Parameters for the Determination of Zinc

The pH of the solution of 5.0 μg L^{-1} of zinc was varied in steps of 0.5 over the range of 8.0 to 11.0 by addition of the 0.1M NH_3-NH_4Cl buffer. SPE of zinc onto C_{18} bonded silica gel was found to be quantitative in the pH range of 9.5–11.0. Therefore, the pH of the sample solution was adjusted to 10.0+0.5 in subsequent studies. SPE of the TAN complex of zinc on C_{18} bonded silica gel was studied at NH_3 concentrations of 0.1–1.0M in steps of 0.1M. No significant influence on the retention efficiency was observed for NH_3 concentrations in the range 0.4–1.0M. Therefore, TAN was prepared in 0.5M NH_3 solutions in subsequent studies. Variation of TAN concentrations in the range of 0.004 to 0.01% did not affect the retention efficiency of zinc on C_{18} bonded silica gel. Therefore, 0.005% TAN was used in the subsequent studies.

Various miscible solvents (acidified to pH ~2.0) such as methanol, dimethyl formamide, dimethyl sulphoxide, and acetonitrile were tested for the elution of zinc, preconcentrated on C_{18} bonded silica gel, by SPE of zinc-TAN complex. Methanol gave the highest absorbance compared to other solvents and was selected for subsequent studies. It was found that nitric acid in the range of 0.01–0.1 mol L^{-1} quantitatively elutes the Zn-TAN chelate complex (extracted during the preconcentration step) on C_{18} bonded silica gel .

Optimization of FIA Flow Conditions

High sample loading flow rates are important for efficient preconcentration and high sample throughput. In general, FI sample flow rates are limited due to the back pressure produced by the column and/or sorption efficiency which decreases with decreasing flow rates. No degradation of sorption efficiency was observed up to a loading flow rate of 10.0 mL/min of the sample and reagent. A higher flow rate through the peristaltic pump and the type of column used in this work will degrade precision. The reagent flow rate should not be too low so as to ensure good mixing of the reagent and sample solutions. Optimum sample and reagent flow rates were found to be 7.0 and 3.0 mL/min, respectively, and these flow rates were used in subsequent experiments.

An elution flow rate of 4.0 mL/min provided optimum sensitivity and elution peaks with minimum tailing. No provision was made to compensate for the lower flow rate delivered by the FI system; however, the transfer capillary to the nebulizer (PTFE, 0.3 mm i.d) restricted the uptake rate to values close to the flow rate provided by the FI system. Operating the nebu-lizer at this flow rate does not lower the sensitivity in proportion to the decrease in flow rate due to the potential improvement in the nebulizer efficiency under starved conditions (19,23). The lower sample flow rate in the FI mode in comparison to the conventional free uptake rate of the nebulizer is also beneficial for droplet diameter distribution, which results in smaller droplets and is therefore less prone to vaporization interferences (23).

Performance of On-line Preconcentration System

The characteristic data for the performance of the on-line preconcentration system is summarized on Table II. The efficiency of SPE was investigated by analyzing the previously collected column eluent from a standard solution of zinc and using the same preconcentration technique. From the results obtained by the repeated preconcentration, a retention efficiency of >99% was calculated for zinc. The SPE elution sequence is highly reproducible, giving an overall precision of 2.5% for five successive determinations of 5.0 μg L^{-1} of zinc (Table II). A linear relationship was observed between preconcentration time and enrichment factor up to a 4-min loading time. With a loading time of 1 min, a 120-fold enhancement in sensitivity compared to conventional flame AAS was observed and the detec-

TABLE II
Analytical Performance Data of Flow Injection On-line Solid Phase Extraction and AAS Determination of Zn

Linear range	0.5–50 μg L^{-1}
Sensitivity enhancement[a]	120
Concentration efficiency[a]	120
Precision (RSD[b]) (at 5 μg L^{-1})	2.5%
Sample consumption	7.0 mL
Loading time	60 s
Sample frequency	30/h
Detection limit (3 σ)	0.15 μg L^{-1}

[a] Compared to conventional nebulization. [b] n = 5.

tion limit corresponding to three times the standard deviation of the blank was found to be 0.15 μg L^{-1} for zinc. The linear equation with regression was as follows :

$$A = 0.00085 + 0.0299C$$

The correlation coefficient was 0.9985 where A is the absorbance and C is the concentration of zinc in μg L^{-1}. All statistical calculations are based on the average of triplicate readings for each standard solution in the given range. Further, a 1-min loading time allows a sampling frequency of 30/h. Higher sensitivities can be obtained by modifying the method, i.e., using a longer preconcentration period at the expense of lower sample throughput.

Interference Studies

The tolerance of maximum concentrations of coexisting ions usually present in soil samples and neutral electrolytes in the determination of 5 μg L^{-1} of zinc was systematically studied using the FIA-AAS procedure described above. Any deviation greater than 3% or more from the standard absorbance value was taken as interference. The maximum concentration of neutral electrolytes and coexisting ions which do not cause reduction in the FIAS-AAS signal of zinc are: NaCl (0.1 M); NaNO$_3$ (0.1 M); Na$_2$SO$_4$ (0.1 M); Fe, Zn, Co, Ni, or Mn (50 μg/mL); and Cr or Mo (200 μg/mL). These observations suggest that the developed procedure can be used for the determination of zinc in soil samples.

Analysis of Soil Samples

Since the coexisting ions and neutral electrolytes do not interfere in the ultra trace determination of zinc, it was decided to analyze the four different fractions of the various soil samples collected from different locations in India. The results obtained by the developed FIAS-AAS procedure using the direct and standard addition methods for zinc are summarized in Table III. The following observations can be deduced:

1. The total amount of zinc present in soil samples varies from 0.185 μg/g (Mango Garden at Stiles, Mangapuram) to 0.991 μg/g (Voltarek Electrodes, G. Mandyam) of soil sample.

2. In all samples, Fraction IV contains considerable amounts of zinc compared to Fractions I, II, and III, indicating that zinc is present not as (a) exchangeable/acetic acid soluble, (b) bound to iron/manganese oxides, or (c) bound to organic matter which is leached under oxidizing conditions.

3. In samples 2, 4, 9, 10, 11, and 12, considerable amounts of zinc are leached in Fraction III, indicating that zinc is bound to organic matter.

4. The zinc content in Fraction II of samples 3 and 4 is not detectable by the present method, indicating the absence of zinc bound to iron/manganese oxides.

5. Only the sample collected near the Grindwell Norton Factory does not contain traces of exchangeable/acetic acid soluble zinc.

CONCLUSION

On-line SPE preconcentration FIAS-FAAS allows the determination of zinc as low as 0.002 μg L^{-1} per g of soil sample with an overall enrichment factor of 120 in 1 min of preconcentration time. The precision of the developed procedure is also good as the RSD value for five successive determinations of zinc in soil samples was found to be in the range 2.5–4.0%. The developed procedure is simple and rapid (sample throughput = 30/h) and allows the determination of 0.5 to 50 μg L^{-1} of zinc by using TAN as the chelating/sorbent extraction agent.

TABLE III. Determination of Zn in Soil Samples ($\mu g\ g^{-1}$) [a]

Sample Description		Acetic Acid Fraction (I)		Hydroxylamine HCl Fraction (II)		H$_2$O$_2$ Fraction (III)		HF + HNO$_3$ Fraction (IV)		Total Zinc	
		Direct	SA	Direct	SA	Direct	SA	Direct	SA	Direct	SA
1. Near Madhu Industries, Agarala		0.06±0.002	0.058±0.002	0.009±0.002	0.010±0.002	0.02±0.002	0.021±0.002	0.117±0.003	0.120±0.003	0.210±0.002	0.215±0.004
2. Near Spartek Ceramics, Mangapuram		0.05±0.002	0.048±0.002	0.039±0.002	0.040±0.002	0.291± 0.004	0.290±0.005	0.062±0.002	0.060±0.002	0.450±0.008	0.450±0.008
3. Near Mango Garden at Stiles India, Mangapuram		0.009±0.002	0.010±0.002	<0.002	<0.002	0.027±0.002	0.025± 0.002	0.144±0.003	0.146±0.003	0.184±0.003	0.185±0.003
4. Mungilipattu Fertile Land		0.029±0.002	0.028±0.002	0.023±0.002	0.022±0.002	0.041± 0.002	0.040±0.002	0.317±0.005	0.320±0.005	0.410±0.008	0.415±0.008
5. Near Sugar Factory, G. Mandyam		0.008±0.002	0.009±0.002	<0.002	<0.002	0.120±0.003	0.122±0.003	0.265±0.004	0.260±0.004	0.405±0.008	0.410±0.008
6. Near Steel Factory		0.008±0.002	0.008±0.002	0.044±0.002	0.040±0.002	0.025±0.002	0.025±0.002	0.430±0.008	0.420±0.009	0.510±0.01	0.50±0.01
7. Near AmaraRaja Batteries		0.081±0.003	0.080±0.003	0.040±0.002	0.040±0.002	0.070±0.003	0.069±0.003	0.128±0.003	0.130±0.003	0.323±0.006	0.320±0.006
8. Near Grindwell Norton Factory		<0.002	<0.002	0.160±0.004	0.158±0.004	0.081±0.003	0.080±0.003	0.392±0.008	0.395±0.008	0.625±0.015	0.630±0.015
9. Near Water Distilleries, G. Mandyam		0.161±0.003	0.160±0.003	0.166±0.004	0.165±0.004	0.213±0.004	0.215±0.004	0.415±0.008	0.410±0.008	0.960±0.020	0.965±0.020
10. Near Voltark Electrodes, G. Mandyam		0.106±0.002	0.105±0.002	0.140±0.003	0.145±0.003	0.319±0.008	0.320±0.008	0.426±0.008	0.425±0.008	0.991±0.020	0.990±0.020
11. Near Mango Garden, Renigunta		0.063±0.002	0.061±0.002	0.094±0.002	0.095±0.002	0.128±0.003	0.130±0.003	0.420±0.008	0.425±0.008	0.704±0.015	0.705±0.015
12. Near S.V. Sugars, G. Mandyam		0.072±0.002	0.075±0.002	0.077±0.002	0.074±0.002	0.138±0.003	0.140±0.003	0.287±0.006	0.285±0.006	0.581±0.015	0.585±0.015

[a] Average of of three determinations.   Direct = Direct method.   SA = Standard addition method.

REFERENCES

1. J. Mary Gladis and T. Prasada Rao, Met. News 21, 24 (2003).

2. A. Junker-Bucheit and M. Witzenbacher, J. Chromatogr. A 737, 67 (1996).

3. J. Mary Gladis and T. Prasada Rao, Anal. Lett. 35, 501 (2002).

4. C.R. Preetha, J. Mary Gladis, and T. Prasada Rao, Talanta 58, 701 (2002).

5. Z. Fang, Flow injection atomic absorption spectrometry, John Wiley & Sons Ltd, West Sussex, England (1995).

6. Z. Fang, Spectrochim. Acta, Part B, 53, 1371 (1998).

7. H. Tuescher and R. Alder, The Soil and its Fertility, Reinhold Publishing Corporation, New York (1960).

8. G. Plaisance and A.Caileux, Dictionary of Soils, Amerind Publishing Co. Pvt. Ltd., pg. 1087, New York (1981).

9. S.J. Hill, Chem. Soc., Rev. 26, 291 (1997).

10. H.F. Pickering, CRC Crit. Rev. Anal. Chem. 12, 233 (1981).

11. H.D. Fiedler, J.F. Lopez-Sanchez, R. Rubio, G. Rauret, Ph. Quevauviller, A.M. Ure, and H. Muntan, Analyst 119, 1109 (1994).

12. B. Marin, M. Valladon, M. Polve, and A. Monaco, Anal. Chim. Acta 342, 91 (1997).

13. J. Fu, G. Liu. J. Yang, Z. Wang, and C. Ma, Huaxue Tongbao 8, 48 (1990).

14. N. Porter, B.T. Hart, R. Morrison, and I.C. Hamilton, Anal. Chim. Acta 281, 229 (1993).

15. E.V. Kirko, N.M. Sorokina, N.N. Galdona, G.I. Trizin, and Yu. A. Zolotov, Zavod. Lab. 62, 26 (1996).

16. T. Yokoyama, T. Watarai, T. Vehara, K.I. Mizouka, K. Kohara, M. Kido, and M. Zenk, Fresenius' J. Anal. Chem. 357, 860 (1992).

17. R. Purohit and S. Devi, Analyst 116, 825 (1991).

18. M. Sperling, P. Koschiechlak, and B. Welz, Anal. Chim Acta 261, 115 (1992).

19. K.A. Tony, S. Karthikeyan, B.Vijayalakshmy, T. Prasada Rao, and C.S.P. Iyer, Analyst 124, 191 (1999).

20. Z. Zhang and X. Zheng, Guangpuxue Yu Guangpu Fenxi 11, 32 (1991).

21. D.M. Ye, H.Q. Zhang, and Q.H. Jin, Talanta 43, 535 (1996).

22. J. Mary Gladis, V.M. Biju, and T. Prasada Rao, At. Spectrosc. 23, 143 (2002).

23. M. Sperling, S. Xu, and B. Welz, Anal. Chem. 64, 3101 (1992).

Determination of Metals in Lubricating Oil
of Electricity Generating Turbines

*F. Hellal[a] and M. Blancou[b]

**[a] Département de Chimie, Institut National des Sciences Appliquées et de Technologie
B.P. 676 - 1080 Tunis cedex, Tunisia**

[b] Laboratoire Central de Chimie à la Société Tunisienne de l'Electricité et du Gaz (S.T.E.G.), Tunisia

INTRODUCTION

A number of methods have been developed by Barras (1), Burrows et al. (2), Fernández et al. (3), and Pignalosa and Knochen (4), etc., for the determination of metals in the organic phase. S.T.E.G. (a Tunisian electric and gas company) uses xylene to determine the metals present in lubricating oil of turbines that generate electricity. The concentration of these metals in the oil indicates the state of the various parts of the turbine. The technique of using xylene was first introduced by Sprague and Slavin (5). At the present time, xylene is classified as a dangerous substance known to cause many diseases such as acceleration of brain damage (6), damage to the respiratory tract (7), and loss of vision (8).

In this paper we describe a new and safe method for the determination of copper, iron, and lead in lubricating oil from turbines that generate electricity in the following experimental domain (Table I):

TABLE I
Experimental Domain

	Lower Limit	Upper Limit
Cu conc. (ppm)	1	7
Fe conc. (ppm)	15	21
Pb conc. (ppm)	2	8
Mixing temp. (°C)	20	25

Corresponding author.
e-mail: hellalf@yahoo.fr

ABSTRACT

S.T.E.G., a Tunisian electric and gas company, uses xylene for the determination of metals in the organic phase. Xylene is a dangerous substance that causes many diseases. In this article, we suggest a new and safe approach that will permit the determination of copper, iron, and lead in lubricating oil used in turbines that generate electricity.

This approach is based on the extraction of metals by hydrochloric acid using mechanical mixers. We developed some mathematical models to predict the concentration of metals from the values of their absorbance, determined in the aqueous phase by atomic absorption spectrometry. It is to be noted that this method does not require the total extraction of the metals and is a more simplified method than those based on the partition coefficient.

METHOD

To correlate the relevant factors (concentration of copper, iron, and lead in the organic phase) to the response (absorbance of copper, iron, and lead in the aqueous phase), we will consider the phenomenon as a dark box (Figure 1) (9–12).

Where,

Y_{Cu} = the response representing the absorbance of copper in the aqueous phase

Y_{Fe} = the response representing the absorbance of iron in the aqueous phase

Y_{Pb} = the response representing the absorbance of lead in the aqueous phase

U_1 = First factor representing the concentration of copper in the organic phase

U_2 = Second factor representing the concentration of iron in the organic phase

U_3 = Third factor representing the concentration of lead in the organic phase

U_4 = Fourth factor representing the mixing temperature.

In order to compare the effects of different factors in the respective experimental domain, coded variables were used. The following equation can transform the factors U_1, U_2, U_3, and U_4 into the coded variables X_1, X_2, X_3, and X_4:

$$X_i = \frac{U_i - \overline{U_i}}{\Delta U_i} \qquad (1)$$

where

X_i = the value taken by the coded variable i

U_i = the value taken by the factor i

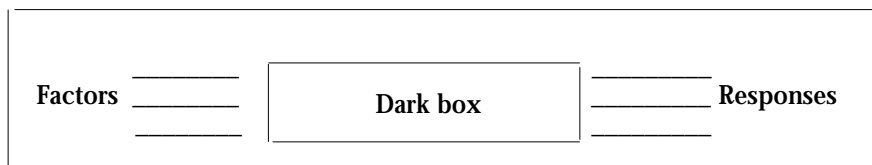$\overline{U_i}$ = the value taken by the factor i in the center of the experimental field concerned

Fig. 1. Adopted approach.

Atomic Spectroscopy
Vol. 24(4), July/August 2003

125

ΔU_i = the range of variation of the factor i.

$$\overline{U_i} = \frac{\text{(Upper limit (U}_i) + \text{lower limit (U}_i)}{2}$$

$$\Delta U_i = \frac{\text{(Upper limit (U}_i) - \text{lower limit (U}_i)}{2}$$

Since there is a low range of variation of the factors, there is a high probability for the following model:

$$Y = b_0 + b_1 X_1 + b_2 X_2 + b_3 X_3 + b_4 X_4 \quad (2)$$

Y=the response representing the absorbance

b_i=represents the estimation of the main effects of the factor i

In matrix form we can write $Y = X B_1$, where Y is the vector of measured response (absorbance), X is the model matrix, and B_1 is the vector of estimates of the coefficients calculated using the least squares method:

$$B_1 = (X^T X)^{-1} X^T Y \quad (3)$$

To calculate the coefficient values of model number 2, we selected the 2^{4-1} fractional factorial design. In this case, the model matrix X contains eight experiments and five columns as shown in Table II.

TABLE II
Model Matrix X

No. of Experiment	X_0	X_1	X_2	X_3	X_4
1	1	-1	-1	1	-1
2	1	1	-1	-1	-1
3	1	-1	1	-1	-1
4	1	1	1	1	-1
5	1	-1	-1	1	1
6	1	1	-1	-1	1
7	1	-1	1	-1	1
8	1	1	1	1	1

EXPERIMENTAL

Instrumentation

A PerkinElmer AAnalyst™ 300 atomic absorption spectrometer was used for this study, equipped with a 10-cm burner for air-acetylene flame and operated with hollow cathode lamps (PerkinElmer Life and Analytical Sciences, Shelton, CT, USA).

Reagents and Standard Solutions

The required concentrations of copper, iron, and lead were prepared in 10-mL volumetric flasks using commercial standard solutions of metals (1000 mg/kg), dissolved in mineral oil (Merck, Darmstadt, Germany). The known volume of standard solutions was taken and then brought to 10-mL volume using lubricating oil from turbines that generate electricity (TERESSO 46).

Ten mL of concentrated hydrochloric acid was added to every 10 mL of lubricating oil of the solution from these turbines containing the quantities of copper, iron, and lead as stated in Table I. The solutions were then mechanically mixed with an agitator (Promax 2020, Prolabo, Paris, France) at a fixed temperature for 30 minutes, as listed in Table I. After a 15-min centrifugation, the acid aqueous phase was separated and diluted three times with demineralized water in order to avoid high concentrations of acid. This solution was then analyzed with the Model AAnalyst 300 atomic absorption spectrometer.

RESULTS AND DISCUSSION

The absorbance values obtained are listed in Table III and the coefficient values of the models are listed in Table IV. The data presented in this manuscript were processed using the Nemrod software program (L.P.R.A.I, Marseille, France) (13).

The results in Table IV show that there is no significant influence of the mixing temperature (b_4) on the absorbance of copper, iron, and lead.

To check the weight of different coefficients, Pareto analysis was performed. Plots of the contribution of every term are displayed in Figures 2, 3, and 4. The percentage effect Pi of every term i was calculated using the Haaland equation as follows (14):

$$P_i = 100 \, (b_i^2 / \Sigma b_j^2) \quad (4)$$

Figures 2, 3, and 4 using the selected experimental parameters show that the main effect on Y_{Cu} is the concentration of copper (P1 = 100%), on Y_{Fe} it is the concentration of iron (P2 = 99.87 %), and on Y_{Pb} it is the concentration of lead

TABLE III
Obtained Absorbance Values of the 2^{4-1} Fractional Factorial Design

No. of Experiment	U_1	U_2	U_3	U_4	Y_{Cu}	Y_{Fe}	Y_{Pb}
1	1	15	8	20	0.0270	0.0250	0.1046
2	7	15	2	20	0.2088	0.0224	0.0012
3	1	21	2	20	0.0270	0.0934	0.0018
4	7	21	8	20	0.2092	0.0964	0.1048
5	1	15	8	25	0.0274	0.0249	0.1049
6	7	15	2	25	0.2090	0.0227	0.0014
7	1	21	2	25	0.0273	0.0943	0.0017
8	7	21	8	25	0.2092	0.0968	0.1052

(P3 = 100%), respectively. In addition we can conclude that the mixing temperature has no significant influence on the three responses Y_{Cu}, Y_{Fe}, and Y_{Pb} as we have (P4 = 0.00 %) in the three cases. Hence, we can reduce the models to:

$$Y_i = b_0 + b_1 X_{1i} + b_2 X_{2i} + b_3 X_{3i} \quad (5)$$

with Y_i the value of the absorbance obtained in experiment number i.

To estimate the coefficients of equation number 5, we need only use the four experiments (numbers 1, 2, 3, and 4) as listed in Table III because they form a 2^{3-1} fractional factorial design :

$$b_0 = (Y_1 + Y_2 + Y_3 + Y_4) / 4 \; ;$$
$$b_1 = (-Y_1 + Y_2 - Y_3 + Y_4) / 4 \; ;$$
$$b_2 = (-Y_1 - Y_2 + Y_3 + Y_4) / 4 \; ;$$
$$b_3 = (Y_1 - Y_2 - Y_3 + Y_4) / 4.$$

$$Y_{Cu} = 0.1180 + 0.0910 X_1 + 0.0001 X_2 + 0.0001 X_3 \quad (6)$$

($R^2 = 1$, F-ratio = 6.1 E+05, P-value = 0.000).

$$Y_{Fe} = 0.0593 + 0.0001 X_1 + 0.0356 X_2 + 0.0014 X_3 \quad (7)$$

($R^2 = 1$, F-ratio = 2.5 E + 04, P-value = 0.000)

$$Y_{Pb} = 0.0531 - 0.0001 X_1 + 0.0002 X_2 + 0.0516 X_3 \quad (8)$$

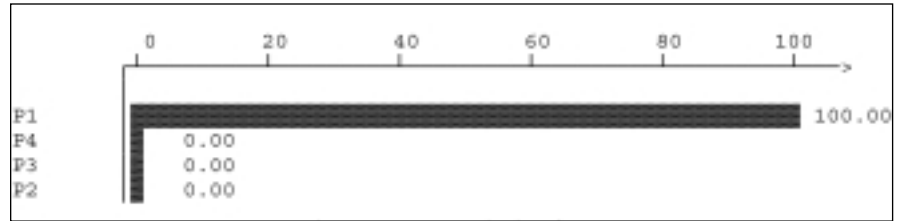($R^2 = 1$, F-ratio = 1.9 E + 05, P-value = 0.000)

Fig. 2. Pareto analysis of Y_{Cu}.

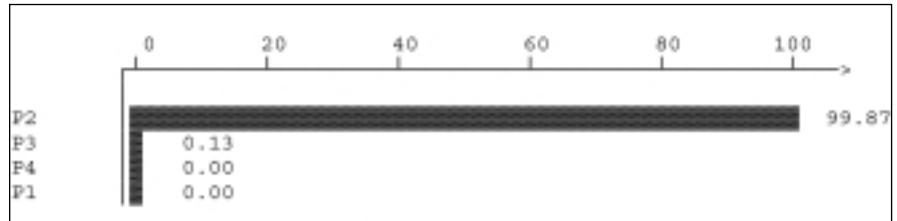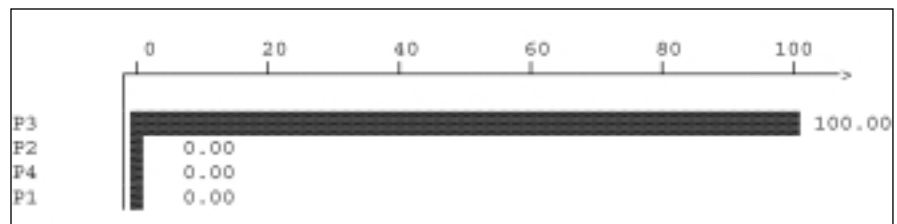

Fig. 3. Pareto analysis of Y_{Fe}.

Fig. 4. Pareto analysis of Y_{Pb}.

Our aim is to determine the concentration of copper (U_1), iron (U_2), and lead (U_3) in the sample before the extraction. Hence, it will be useful to formulate equation models (#6), (#7) and (#8) as follows:

In the first step, application of equation (#1) allows us to change the coded variables X_i by the concentration U_i:

$$Y_{Cu} = -0.00410 + 0.03033 U_1 + 0.00003 U_2 + 0.00003 U_3 \quad (9)$$

$$Y_{Fe} = -0.15677 + 0.00003 U_1 + 0.01187 U_2 + 0.00047 U_3 \quad (10)$$

$$Y_{Pb} = -0.03397 - 0.00003 U_1 + 0.00007 U_2 + 0.01720 U_3 \quad (11)$$

TABLE IV.   Models of Coefficient Values

	Y_{Cu}				Y_{Fe}				Y_{Pb}			
	Coefficient	Standard	t_{exp}	Signif.	Coefficient	Standard	t_{exp}	Signif.	Coefficient	Standard	t_{exp}	Signif.
b_0	0.11811	0.00004	2800	***	0.05949	0.00010	578.5	***	0.05320	0.00005	985.1	***
b_1	0.09094	0.00004	2100	***	0.00009	0.00010	0.85	0.46	−0.00005	0.00005	−0.9	0.425
b_2	0.00006	0.00004	1.5	0.239	0.03574	0.00010	347.5	***	0.00018	0.00005	3.2	*
b_3	0.00009	0.00004	2.1	0.132	0.00129	0.00010	12.6	***	0.05167	0.00005	956.8	***
b_4	0.00011	0.00004	2.6	0.077	0.00019	0.00010	1.8	0.165	0.00010	0.00005	1.9	0.161
R^2	1				1				1			
F-ratio	1.1 E+06				3.0 E+04				2.3 E+05			
P-value	0.000				0.000				0.000			

We can write these models in matrix form as follows:

$$\begin{bmatrix} Y_{Cu} + 0.00410 \\ Y_{Fe} + 0.15677 \\ Y_{Pb} + 0.03397 \end{bmatrix} = \begin{bmatrix} 0.03033 & 0.00003 & 0.00003 \\ 0.00003 & 0.01187 & 0.00047 \\ -0.00003 & 0.00007 & 0.01720 \end{bmatrix} \begin{bmatrix} U_1 \\ U_2 \\ U_3 \end{bmatrix} = B_2 \begin{bmatrix} U_1 \\ U_2 \\ U_3 \end{bmatrix}$$

In the second step, we can have:

$$\begin{bmatrix} U_1 \\ U_2 \\ U_3 \end{bmatrix} = B_2^{-1} \begin{bmatrix} Y_{Cu} + 0.00410 \\ Y_{Fe} + 0.15677 \\ Y_{Pb} + 0.03397 \end{bmatrix}$$

This can be arranged in the following form:

$$U_1 = 0.115 + 32.967 \, Y_{Cu} - 0.092 \, Y_{Fe} - 0.062 \, Y_{Pb} \tag{12}$$

$$U_2 = 13.135 - 0.095 \, Y_{Cu} + 84.283 \, Y_{Fe} - 2.287 \, Y_{Pb} \tag{13}$$

$$U_3 = 1.924 + 0.064 \, Y_{Cu} - 0.327 \, Y_{Fe} + 58.148 Y_{Pb}. \tag{14}$$

To test the validity of these models, we have selected the test points given in Table V and determined the absorbance values according to the experimental protocol described in the Experimental section. We aimed to recover the entire experimental domain with these test points.

In comparing the predicted concentration values, calculated using equation models (#12), (#13), and (#14), with the real concentration values, no significant difference was found (see Table VI); thus, these results confirm the validity of our assumptions.

Estimation of Interaction and Square Terms

The selected experiments (numbers 1, 2, 3, 4, T6, T7, T8 and T9) form a factorial design 2^3, which offers the possibility to calculate the coefficients of equation model (#15):

$$Y = b_0 + b_1 X_1 + b_2 X_2 + b_3 X_3 + b_{12} X_1 X_2 + b_{13} X_1 X_3 + b_{23} X_2 X_3 + b_{123} X_1 X_2 X_3 \tag{15}$$

where Y is the response representing the absorbance; b_i is the estimation of the main effect of the factor i ; b_{12}, b_{13}, and b_{23} are the estimation of the interactions between copper and iron, copper

TABLE V.   Selected Test Points and Obtained Experimental Results

No. of Experiment	X_1	X_2	X_3	U_1	U_2	U_3	Y_{Cu}	Y_{Fe}	Y_{Pb}
T5	0	0	0	4.01	18.02	5	0.1178	0.0603	0.0531
T6	-1	-1	-1	1.06	15.02	2.09	0.0288	0.0234	0.0030
T7	1	1	-1	6.96	20.97	2.07	0.2081	0.0932	0.0031
T8	1	-1	1	6.98	15.00	7.95	0.2083	0.0249	0.1039
T9	-1	1	1	1.03	20.96	7.98	0.0276	0.0961	0.1051
T10	0	0	0	4.03	18.04	5.02	0.1188	0.0595	0.0531
T11	-0.5	-0.5	-0.5	2.52	16.48	3.48	0.0728	0.0409	0.0268
T12	0.5	-0.5	-0.5	5.49	16.50	3.49	0.1633	0.0407	0.0269
T13	-0.5	0.5	-0.5	2.48	19.48	3.52	0.0723	0.0762	0.0278
T14	0.5	0.5	-0.5	5.47	19.53	3.50	0.1634	0.0768	0.0270
T15	-0.5	-0.5	0.5	2.45	16.52	6.51	0.0708	0.0415	0.0791
T16	0.5	-0.5	0.5	5.48	16.51	6.52	0.1629	0.0420	0.0791
T17	-0.5	0.5	0.5	2.49	19.47	6.52	0.0718	0.0774	0.0790
T18	0.5	0.5	0.5	5.49	19.51	6.48	0.1632	0.0777	0.0791
T19	0	0	0	3.98	17.98	4.99	0.1171	0.0592	0.0529

* Because of the experimental conditions, we tried to have the factor values (U_i) as close as possible to the coded variable values (X_i).

and lead, and iron and lead, respectively, and finally b_{123} is the estimation of the interaction between copper, iron, and lead.

If we use the experiment numbers 1, 2, 3, 4, T5 to T19 to calculate these model coefficients, we obtain the results shown in Table VII.

We can conclude from the results listed in Table VII that there is no significant interaction between the concentrations of metals in the selected experimental domain. Generally, in order to make a decision about the state of something one requires a critical value but one does not need a large experimental domain. If we take the critical value as the center of the experimental domain and if we select a low range of variation around this value, there is a high probability of finding a linear model. In this case, there is no need to include the interaction and square terms in the model. However, if we find a big difference between the predicted and the real values in the center of the experimental domain, then we can correct the model by adding the interaction and (or) the square terms.

TABLE VI.   Differences Between Values of Real Conc. (U_{iR}) and Calculated Conc. (U_{iC})

	U_{1R}	U_{2R}	U_{3R}	U_{1C}	U_{2C}	U_{3C}	ΔU_1	ΔU_2	ΔU_3
T5	4.01	18.02	5.00	3.99	18.08	5.00	0.02	−0.06	0.00
T6	1.06	15.02	2.09	1.06	15.10	2.09	−0.00	−0.08	−0.00
T7	6.96	20.97	2.07	6.97	20.96	2.09	−0.01	0.01	−0.02
T8	6.98	15.00	7.95	6.97	14.98	7.97	0.01	0.02	−0.02
T9	1.03	20.96	7.98	1.01	20.99	8.01	0.02	−0.03	−0.03
T10	4.03	18.04	5.02	4.02	18.02	5.00	0.01	0.02	0.02
T11	2.52	16.48	3.48	2.51	16.51	3.47	0.01	−0.03	0.01
T12	5.49	16.50	3.49	5.49	16.49	3.49	−0.00	0.01	0.00
T13	2.48	19.48	3.52	2.49	19.49	3.52	−0.01	−0.01	−0.00
T14	5.47	19.53	3.50	5.49	19.53	3.48	−0.02	−0.00	0.02
T15	2.45	16.52	6.51	2.44	16.44	6.51	0.01	0.08	−0.00
T16	5.48	16.51	6.52	5.48	16.48	6.52	0.00	0.03	−0.00
T17	2.49	19.47	6.52	2.47	19.47	6.50	0.02	−0.00	0.02
T18	5.49	19.51	6.48	5.48	19.49	6.51	0.01	0.02	−0.03
T19	3.98	17.98	4.99	3.97	17.99	4.99	0.01	−0.01	0.00

TABLE VII.   Obtained Results

	Y_{Cu}				Y_{Fe}				Y_{Pb}			
	Coeff.	Standard	t_{exp}	Signif.	Coeff.	Standard	t_{exp}	Signif.	Coeff.	Standard	t_{exp}	Signif.
b_0	0.1180	0.0001	1700	***	0.0593	0.0001	669.12	***	0.0531	0.0001	821.77	***
b_1	0.0911	0.0001	9.24	***	−0.0001	0.0001	−0.70	0.504	−0.0001	0.0001	−0.67	0.522
b_2	0.0001	0.0001	1.15	0.276	0.0356	0.0001	290.39	***	0.0002	0.0001	2.25	*
b_3	−0.0001	0.0001	−1.12	0.287	0.0012	0.0001	10	***	0.0517	0.0001	575.97	***
b_{12}	0.0001	0.0001	1.28	0.226	0.0001	0.0001	0.60	0.567	−0.0000	0.0001	−0.39	0.705
b_{13}	0.0000	0.0001	0.24	0.812	0.0001	0.0001	0.51	0.626	−0.0000	0.0001	−0.06	0.954
b_{23}	−0.0001	0.0001	−1.08	0.303	0.0002	0.0001	1.74	0.106	−0.0000	0.0001	−3.13	0.892
b_{123}	0.0000	0.0001	0.15	0.879	−0.0001	0.0001	−1.01	0.338	−0.0001	0.0001	−1.20	0.256
R^2	1				1				1			
F-ratio		1.2 E+05				1.2 E+04				4.7 E+04		
P-value		0.000				0.000				0.000		

Study of Error Propagation

An important relationship exists between the relative error in the analytical result ($||\Delta U|| / ||U||$) and the relative error in the measurements ($||\Delta Y|| / ||Y||$) (15–17), namely:

$$\frac{||\Delta U||}{||U||} \leq ||K|| \cdot ||K^{-1}|| \left\{ \frac{||\Delta Y||}{||Y||} + \frac{||\Delta K||}{||K||} \right\} \tag{16}$$

The K-matrix of the analytical system given in equations (#9), (#10), and (#11) is:

$$K = \begin{bmatrix} 0.03033 & 0.00003 & 0.00003 \\ 0.00003 & 0.01187 & 0.00047 \\ -0.00003 & 0.00007 & 0.01720 \end{bmatrix}$$

Because, in most cases, the relative error in the K values is much smaller than the relative error in the measurements, equation (#16) becomes:

$$\frac{||\Delta U||}{||U||} \leq COND\ (K)\ \frac{||\Delta Y||}{||U||} \tag{17}$$

Where $COND\ (K) = ||\ K\ || \cdot ||\ K^{-1}\ || \tag{18}$

COND (K) relates to the relative magnitude of the different sensitivity coefficients in the K-matrix, with the amplification of the measurement error into the analytical result.

As the matrix K is square, the norm of K, $||\ K\ ||$, equals λ_1, which is the largest Eigenvalue of K. It can be derived that the norm of the inverse matrix K^{-1}, $||K^{-1}||$, is the reciprocal value of the smallest Eigenvalue of K, i.e., $1/\lambda_m$ (17, 18). Then we have:

$$\frac{||\Delta U||}{||U||} \leq 2.6\ \frac{||\Delta Y||}{||Y||} \tag{19}$$

This means that the relative error in the analytical result is not very far from the relative error in the measurement. If we repeat the experiment in the center of the experimental domain six times (Table VIII), we find:

$$||\Delta Y|| / ||Y|| = 0.0032 \text{ and } ||\Delta U|| / ||U|| = 0.0014.$$

$$[||\Delta U|| / ||U|| = 0.4\ ||\Delta Y|| / ||Y||] \leq 2.6\ ||\Delta Y|| / ||Y||$$

This means that the error has been amplified by a factor of 0.4, while from COND (K) = 2.6, a maximal error amplification up to a factor of 2.6 was expected.

TABLE VIII. Values of Real Conc. (U_{iR}) and Calculated Conc. (U_{iC}) for Six Experiments in the Center of the Experimental Domain

No. of Replication	U_{1R}	U_{2R}	U_{3R}	Y_{Cu}	Y_{Fe}	Y_{Pb}	U_{1C}	U_{2C}	U_{3C}
R1	4.00	18.00	5.00	0.1177	0.0593	0.0532	3.99	18.00	5.01
R2	4.00	18.00	5.00	0.1176	0.0595	0.0532	3.98	18.02	5.01
R3	4.00	18.00	5.00	0.1184	0.0596	0.0534	4.01	18.02	5.02
R4	4.00	18.00	5.00	0.1183	0.0592	0.0529	4.01	17.99	4.99
R5	4.00	18.00	5.00	0.1180	0.0596	0.0528	4.00	18.03	4.98
R6	4.00	18.00	5.00	0.1182	0.0591	0.0530	4.00	17.98	4.99

Comparison Between Proposed Method and Use of Partition Coefficients

If W mL of lubricating oil contains U_1 ppm of copper, extracted with L mL of hydrochloric acid, and U_{1e} ppm of copper is extracted, then U_{1e}/L = concentration of copper remains in the extracting phase and $(U_1 - U_{1e})/W$ = concentration remains in the original solution. The partition coefficient P can be calculated by the formula given by Leo et al. (19) as:

$$P = [(U_1 - U_{1e})/W) / (U_{1e}/L)] \quad (20)$$

If P is constant, we can predict the metals concentration in lubricating oil by knowing the concentration of copper in the extraction phase. The values of the partition coefficients of the samples selected in Tables III and V are listed in Table IX. The variation of Y_{Cu}, P, and Log P versus the concentration of copper is represented in Figure 5.

$$Y_{Cu} = 0.0304 \, U_1 - 0.0035$$
$$(R^2 = 1, \text{F-ratio} = 883815,$$
$$\text{P-value} = 0.000) \quad (21)$$

$$P = 0.0051 \, U_1^2 - 0.0579 \, U_1 + 0.2109 \quad (R^2 = 0.9534,$$
$$\text{F-ratio} = 162,$$
$$\text{P-value} = 0.000) \quad (22)$$

$$\text{Log P} = 0.0174 \, U_1^2 - 0.2191 \, U_1 - 0.5976$$
$$(R^2 = 0.9778, \text{F-ratio} = 352,$$
$$\text{P-value} = 0.000) \quad (23)$$

As shown by equations (#21), (#22), and (#23), the value of P is not constant. The simplest model and the best correlation is obtained with Y_{Cu}. Hence, the probability of obtaining better results using the proposed method is higher than with methods that use the partition coefficients.

TABLE IX. Values of Partition Coefficients

|	U_1	U_2	U_3	Y_{Cu}	P	Log P
1	1	15	8	0.0270	0.1629	−0.7880
2	7	15	2	0.2088	0.0527	−1.2785
3	1	21	2	0.0270	0.1629	−0.7880
4	7	21	8	0.2092	0.0506	−1.2954
T5	4.01	18.02	5	0.1178	0.0689	−1.1620
T6	1.06	15.02	2.09	0.0288	0.1557	−0.8078
T7	6.96	20.97	2.07	0.2081	0.0502	−1.2996
T8	6.98	15.00	7.95	0.2083	0.0522	−1.2825
T9	1.03	20.96	7.98	0.0276	0.1718	−0.7650
T10	4.03	18.04	5.02	0.1188	0.0651	−1.1861
T11	2.52	16.48	3.48	0.0728	0.0869	−1.0610
T12	5.49	16.50	3.49	0.1633	0.0556	−1.2548
T13	2.48	19.48	3.52	0.0723	0.0770	−1.1132
T14	5.47	19.53	3.50	0.1634	0.0511	−1.2913
T15	2.45	16.52	6.51	0.0708	0.0866	−1.0627
T16	5.48	16.51	6.52	0.1629	0.0563	−1.2496
T17	2.49	19.47	6.52	0.0718	0.0889	−1.0510
T18	5.49	19.51	6.48	0.1632	0.0563	−1.2497
T19	3.98	17.98	4.99	0.1171	0.0672	−1.1726
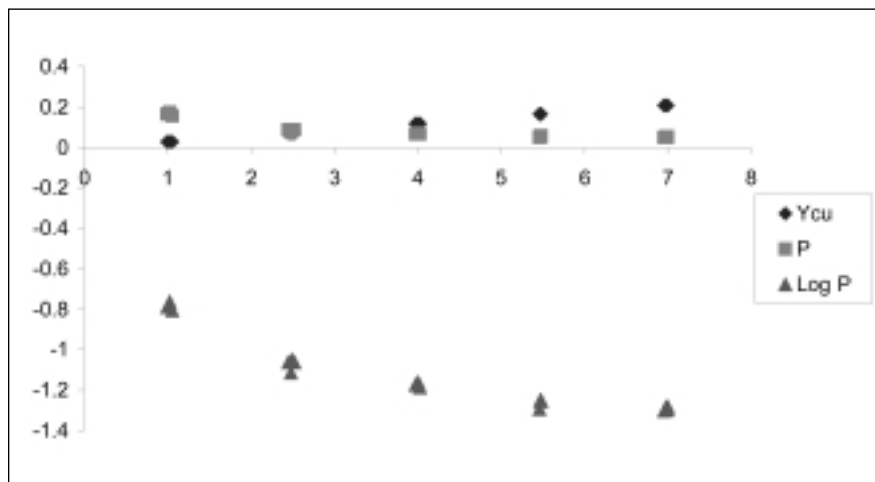
Fig. 5. Variation of Ycu, P, and Log P versus the concentrations of copper.

Comparison Between Proposed Method and Use of Xylene

To compare the method proposed to the method where xylene is used, we selected 10 samples from Table V (T10 to T19); the results are listed in Table X. Since we are not able to assume that the results for the xylene method are normally distributed in the chosen experimental domain, we opted to use the Wilcoxon T-test.

We found a calculated T value equal to 24, 22, and 25 for copper, iron, and lead, respectively. In the three cases, the calculated T value is upper than the critical value of T equal to 8. Hence, we can conclude

TABLE X. Values of Calculated Conc by Proposed Method (U_{iC}) and Conc Found Using Xylene (U_{ixy})

No. of Experiment	U_{1C}	U_{2C}	U_{3C}	U_{1xy}	U_{2xy}	U_{3xy}	Δ_{U1}	Δ_{U2}	Δ_{U3}
T10	4.02	18.02	5.00	3.98	17.81	4.75	0.05	0.23	0.27
T11	2.51	16.51	3.47	3.10	17.10	3.76	−0.58	−0.62	−0.28
T12	5.49	16.49	3.49	4.50	17.35	3.45	0.99	-0.85	0.04
T13	2.49	19.49	3.52	3.40	18.71	3.93	−0.92	0.77	−0.41
T14	5.49	19.53	3.48	4.60	18.59	4.01	0.87	0.94	−0.51
T15	2.44	16.44	6.51	3.20	17.05	5.57	−0.75	−0.53	0.94
T16	5.48	16.48	6.52	4.53	16.92	5.71	0.95	−0.41	0.81
T17	2.47	19.47	6.50	3.02	18.49	7.23	−0.53	0.98	−0.71
T18	5.48	19.49	6.51	5.01	18.82	7.02	0.48	0.69	−0.54
T19	3.97	17.99	4.99	3.99	18.35	4.81	−0.01	−0.37	0.18

that with this sample size and at a significance level of 5%, there is no difference in the results of the two methods.

CONCLUSION

In this paper, we have developed mathematical models for predicting the concentration of copper, iron, and lead in lubricating oil of turbines that generate electricity. The sample was extracted using concentrated hydrochloric acid (1:1 v/v). The aqueous phase was diluted three times and analyzed by atomic absorption spectrometry for determining the absorbance of copper, iron, and lead (Y_{Cu}, Y_{Fe}, and Y_{Pb}). The proposed method is much simpler than methods based on partition coefficients. It is also important to note that this method does not require the total extraction of the metals and requires only four experiments to obtain the three equations (#12), (#13), and (#14). The low number of experiments makes this approach very useful and efficient. In addition, this method can be adapted and used in other organic phases and experimental domains.

REFERENCES

1. R. C. Barras, Jarrell Ash Newsletter, 13 (1962).
2. J. A. Burrows, J. C. Heerdt and J. B. Willis, Anal. Chem. 37 (1965).
3. V. Fernández-Pérez, M. M. Jiménez-Carmona and M. D. Laque de Castro, Anal. Chim. Acta 433 (1), 47 (2001).
4. G. Pignalosa and M. Knochen, At. Spectrosc. 22 (1), 250 (2001).
5. S. Sprague and W. Slavin, At. Abs. Newsl. 12 (1963).
6. S. Gralewez, D. Wiaderna, and T. Tomas, Int. J. Ocup. Med. Environ. Health. 8(4), 347 (1995).
7. J.W. Foy, D.M. Silverman, and R.N. Schatz, J. Toxical. Environ. Health. 47(2), 135 (1996).
8. E.A. Ansari, Hum. Exp. Toxical. 16(15), 273 (1997).
9. F.Hellal, These, University of Aix-Marseille III, France (1993).
10. F. Hellal, R. Phan-Tan-Luu, and A.M. Siouffi, Analusis 24, 127 (1996).
11. F. Hellal, M. Benna, and M.S. Medimagh, Inter. J. Environmental Studies, 55, 53 (1998).
12. G. A. Lewis, D. Mathieu, and R. Phan-Tan-Luu, Pharmaceutical Experimental Design, Marcel Dekker, New York (1998).
13. D. Mathieu, J. Nony, and R. Phan-Tan-Luu, New Efficient Methodology for Research using Optimal Design (NEMROD) Software-L.P.R.A.I, Marseille, France (1998).
14. P. D. Haaland, Experimental Design in Biotechnology, Marcel Dekker, New York (1989).
15. C. Jochum, P. Jochum, and B. R. Kowalski, Anal. Chem. 53, 85 (1981).
16. J. Stoer, Einführung in die Numerische Mathematik, Springer Verlag, Berlin, Germany (1972).
17. D.L. Massart, B.G.M. Vandeginste, S.N. Deming, Y. Michotte, and L. Kaufman, Chemometrics : A Textbook, Elsevier, Amsterdam (1988).
18. H. Kaiser, Z. Anal. Chem. 260, 252 (1972).
19. A. Leo, C. Hansch, and D. Elkins, Chemical Reviews 71, 6 (1971).

Comparison of Effects of Four Acid Oxidant Mixtures in the Determination of Lead in Foods and Beverages by Hydride Generation-ICP-OES*

Julieta Marrero[a], Sebastián Pérez Arisnabarreta[a], and **Patricia Smichowski[b]

[a] Unidad Proyectos Especiales de Suministros Nucleares, Comisión Nacional de Energía Atómica
Av. Libertador 8250, C1429BNP-Buenos Aires, Argentina

[b] Unidad de Actividad Química, Centro Atómico Constituyentes, Comisión Nacional de Energía Atómica
Av. Gral. Paz 1499, B1650KNA-San Martín, Pcia. de Buenos Aires, Argentina

ABSTRACT

A comparative study was undertaken to evaluate the effects of acetic, citric, nitric, and tartaric acids on the continuous hydride generation of lead using ammonium persulfate as oxidant agent. Inductively coupled plasma optical emission spectrometry (ICP-OES) was used for detection. The operating conditions (chemical and physical parameters) and the concentrations of the acids studied were optimized for the generation of PbH_4 (plumbane). Analytical figures of merit including detection limit, precision, and linear dynamic range are given for the four systems employed. The detection limits for Pb ranged between 4.4 and 6.8 μg L^{-1} depending on the acid used to generate plumbane.

Compared to conventional continuous nebulization on a radial ICP, the present coupling gives a sensitivity increase of a factor of approximately two orders of magnitude. The interferent effect of transition metals (Al, Cd, Co, Cu, Cr, Fe, Mn, Mo, Ni, V, and Zn), other hydride-forming elements (As, Bi, Ge, Sb, Se, Sn, and Te,) and Hg upon the Pb signal using the different acids studied were evaluated. Nickel, Se, and Te are the elements that more severely affect plumbane generation in the four systems tested. Plumbane was produced with 85% efficiency in tartaric acid; also a better control of interferences was observed. Method validation was achieved using two certified reference materials, MURST-ISS-A2 (Antarctic Krill) and CRM 063R (Skim Milk Powder), for which reasonable agreement between certified and measured values for lead content was obtained.

The proposed method was applied to the determination of Pb at μg g^{-1} and μg L^{-1} levels in foods and beverages, respectively. The determination of Pb in these kinds of samples is of high toxicological relevance.

INTRODUCTION

Lead is a non-essential and low abundant element that is ranked at about the 36th place of the elements in the earth's crust (1). In contrast, its specific physical and chemical properties prompted the development of a variety of industrial applications and, as a result, large amounts of Pb have been released into the environment during the last fifty years. As a consequence, there is a health risk for plants, animals, and humans due to the element's potential toxicity. For this reason, an increasing interest exists in developing more sensitive, selective, and reliable analytical methods for the determination of Pb at trace levels in environmental and biological matrices.

Electrothermal atomic absorption spectrometry (ETAAS) is a useful and frequently employed technique for trace and ultra-trace determination of heavy metals. In the specific case of lead, severe matrix effects occur when real samples are analyzed and numerous interferences have been reported (2). Hydride generation (HG) combined with atomic absorption spectrometry (AAS) (3,4), direct current plasma (DCP) (5), inductively coupled plasma optical emission spectrometry (ICP-OES) (6), and ETAAS (7) has been used for the determination of Pb at trace levels and represents an alternative method of interest. In spite of this, there are a series of problems associated to plumbane (PbH_4) generation such as rather low chemical yield of Pb hydride, slow kinetics of reduction, the possibility of reduction of Pb to the elemental state, and instability of the volatile hydride.

Several studies have demonstrated that plumbane was generated with a better efficiency from Pb(IV) rather than from Pb(II) (7). In this context, pre-oxidation to its metastable, tetravalent oxidation state is necessary immediately before hydride generation in order to increase sensitivity and to accelerate the reaction kinetics. In a 1976 paper by Fleming and Ide (8), the generation of plumbane in the presence of $K_2Cr_2O_7$ and tartaric acid was reported for the first time. Even when it is recognized that Pb hydride can only be generated in the presence of strong oxidants, there are different hypotheses on the mode of action of the oxidants. Castillo and co-workers (9) examined the effects of different oxidant agents such as $Ce(SO_4)_2$, H_2O_2, $Na_2S_2O_8$ and $KMnO_4$ on plumbane

generation. Madrid et al. (10) evaluated the effects of different acids on the efficiency of Pb hydride in the potassium dichromate oxidant medium.

The generation of plumbane has been achieved in different combinations of acidic oxidizing media. Potassium dichromate was used with tartaric (8), malic (11), and lactic (12) acids. Hydrogen peroxide was employed in conjunction with citric (10), nitric (14), and perchloric acids (9). Ammonium persulfate was another effective oxidant extensively used for Pb hydride generation in conjunction with nitric acid (10,12,13,14). The use of non-aqueous media has also been examined (15,16). Valdes-Hevia y Temprano et al. (17) reported that the addition of different types of ordered media, including normal micelles and vesicles, was beneficial to increase the sensitivity and to improve the kinetics of the reaction. Madrid and Cámara (18) authored a comprehensive review on lead hydride generation AAS as an alternative to electrothermal AAS methods.

Considering the difficulties associated with plumbane generation, it was deemed of interest to investigate further the different combinations of reaction media. The effect of acetic, citric, nitric, and tartaric acids (at different concentrations) on plumbane generation efficiency was evaluated. $(NH_4)_2S_2O_8$ was chosen as the oxidizing agent, which is considered to be the most efficient and strong oxidant for lead hydride generation. The influence exerted by the media tested on the reduction of the potential interferents (transition metals and other hydride-forming elements) was also evaluated. The method was applied to the determination of Pb in foods and beverages.

EXPERIMENTAL

Instrumentation

Determinations were performed with a Model Plasma 400 sequential ICP-OES (PerkinElmer Life and Analytical Sciences, Shelton, CT, USA). The instrument was equipped with a pneumatic cross-flow nebulizer and a demountable quartz torch. The operating conditions are shown in Table I. The continuous manifolds used to generate lead hydride were based on the use of an eight-channel Minipuls™ 3 peristaltic pump (Gilson, Villiers Le Bel, France) and a U-tube liquid separator. Tygon® tubing of 1.6 mm (i.d.) was used in the peristaltic pump. Two gas-liquid separators (GLS1 and GLS2) were examined. In both systems, the spray chamber was disconnected and replaced with glass tubing to connect the phase separator with the torch. The transfer lines were short enough to avoid transport losses. Details of the gas-liquid separators employed are illustrated in Figure 1.

GLS1: A conventional hydride generator of a sample delivery system (peristaltic pump) at 1.5 mL min^{-1}, a cylindrical glass cell (i.d. 2.5 cm), and a gas-liquid separator was tested in a first stage for plumbane generation. Generated plumbane was swept out by Ar (0.75 L min^{-1}) which was introduced through the other entrance tube. The superior tube was connected directly to the inlet tube of the plasma torch.

GLS2: In this case, the generation cell evaluated was similar to that described by Sturgeon et al. (19) with an internal diameter of 3.8 cm. The acidified sample solution and the reductant were delivered continuously and separately by a peristaltic pump through a Y-glass tube of 2 mm i.d. at a flow rate of 1.5 mL min^{-1} and inserted into the glass cell. An Ar flow rate of 0.75 L min^{-1} was introduced

TABLE I
Plasma 400 ICP-OES Optimized Working Conditions for HG-ICP-OES Coupling

Plasma Conditions

Forward RF power	1.1 kW
Frequency of RF generator	40 MHz
Coolant (outer) gas flow rate	15 L min^{-1}
Auxiliary (intermediate) gas flow rate	2 L min^{-1}
Sample (aerosol) gas flow rate	0.58 L min^{-1}
Analytical wavelength	Pb(I): 220.353 nm
Viewing height above load coil	15 mm
Integration time	20 s
Viewing mode	Radial

Hydride Generation Conditions

Samples and reagents flow rate	2.0 mL min^{-1}
Sample acidity	0.07 mol L^{-1} (tartaric acid)
NaBH$_4$ conc.	2.5 % (m/v)
$(NH_4)_2S_2O_8$	4% (m/v)
Tube size for sample and reductant	1.1 mm (i.d.)

through a side arm that penetrates 12 cm into the cell.

A PerkinElmer® Model 5100 ZL atomic absorption spectrometer, equipped with a Model THGA™ graphite furnace, AS-71 autosampler, and a longitudinal Zeeman-effect background corrector, was used for the study of efficiency. A PerkinElmer electrodeless discharge lamp (EDL) was used as the source of radiation. Pyrolytically coated graphite tubes with pyrolytic graphite L'vov platforms were employed. High purity Ar (flow rate: 300 mL min^{-1}) was employed to purge air from the
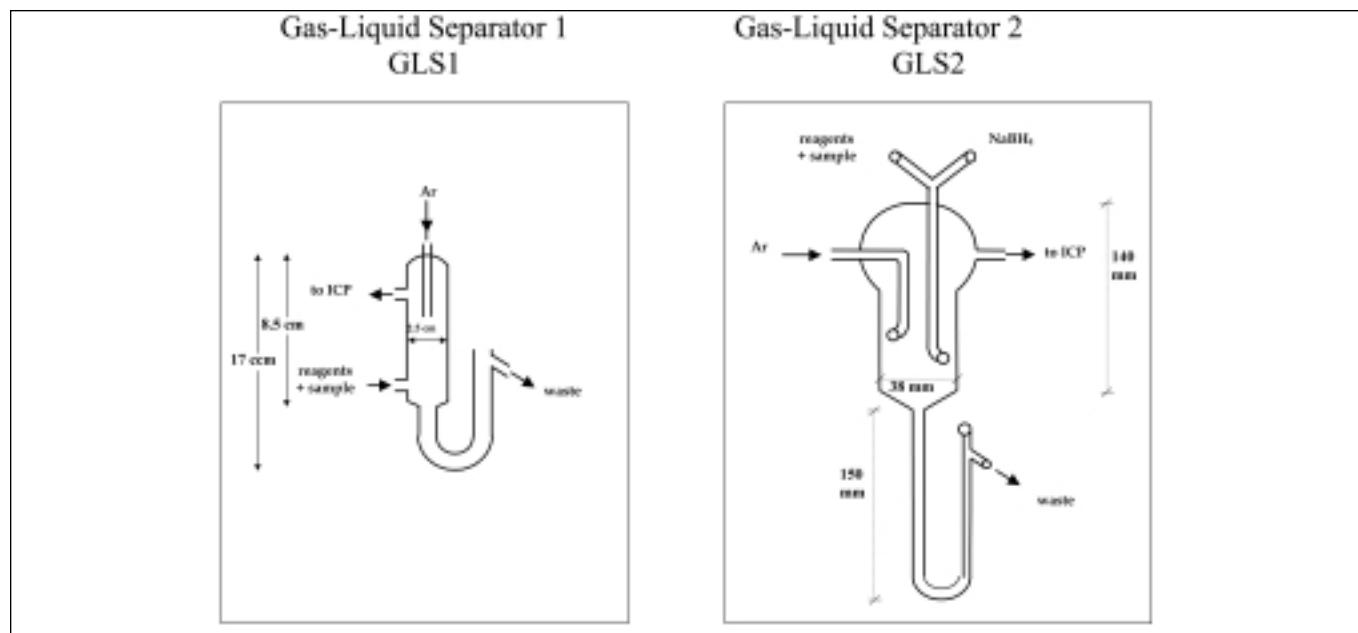
Fig. 1. Schematic diagram of the gas-liquid separators (GLS1 and GLS2) evaluated.

graphite tubes, except during the atomization step, where stopped-flow conditions were used. Autosampler volumes of 20 µL of sample, followed by 5 µL of chemical modifier [5 µg Pd and 3 µg $Mg(NO_3)_2$], were employed. The graphite furnace temperature program used for Pb determination is summarized in Table II.

A Model MLS-2000 microwave apparatus (Milestone-FKW, Sorisole, Bergamo, Italy), equipped with Teflon® vessels, was used to digest the samples.

Reagents and Standard Solutions

Welding argon from Praxair (Buenos Aires, Argentina) was found to be sufficiently pure for Pb determination. All reagents were of analytical reagent grade unless otherwise stated. Deionized distilled water (DDW) was produced by a commercial mixed-bed ion-exchange system (Barnstead, Dubuque, IA, USA), fed with distilled water.

Table II
Graphite Furnace Temperature Program

Parameters	Drying	Pyrolysis	Atomization	Conditioning
Temperature (ºC)	1st Step: 110 2nd Step: 130	1000	2200	2400
Ramp time (s)	1st Step: 1 2nd Step: 15	10	0	1
Hold time (s)	1st Step: 30 2nd Step: 30	20	5	2
Ar flow rate (mL min^{-1})	300	300	0 (read)	300

A commercially available 1000 mg L^{-1} Pb standard solution (Merck, Darmstadt, Germany) was used. Working solutions were prepared daily by serial dilutions of this stock solution. Sodium tetrahydroborate (III) solutions of concentrations ranging from 1 to 3.5% (m/v) were prepared by dissolving NaBH$_4$ powder (Baker, Phillipsburg, NJ, USA) in deionized water and stabilizing in 0.1% (m/v) NaOH (Merck). The solutions were filtered through a Whatman No. 42 filter paper before use to eliminate turbidity. All solutions containing the acids studied

were prepared at the required concentrations by dissolving appropriate amounts of each compound in deionized water or by dilution. Solutions of As, Bi, Cd, Co, Cr, Cu, Fe, Ge, Hg, Mn, Mo, Ni, Sb, Se, Sn, Te, V, and Zn used in this study of interferences were prepared from analytical reagent grade chemicals.

During analytical method development, the concentration of Pb in the test solutions was maintained at 0.5 µg mL^{-1}.

Sample Preparation

Food Samples

Solutions of the samples analyzed were prepared by acid-assisted microwave (MW) digestion. Various combinations and concentrations of acids were investigated for the different kinds of samples analyzed and the mixture selected is detailed in Table III. Before MW treatment, the samples were pre-digested overnight.

The average MW power applied during the digestion cycle varied from 250 to 600 W. In all cases, the duration of the complete cycle was less than 20 min. After cooling, the pressure inside the vessels was vented in the hood. Then, the vessels were opened and placed on a programmable hot plate and evaporated to dryness. The digests were dissolved in 10 mL of 70×10^{-3} mol L^{-1} tartaric acid. The solutions were filtered and transferred into 25-mL volumetric flasks and diluted to the mark with 70×10^{-3} mol L^{-1} tartaric acid. Two portions were prepared for each sample. Blank solutions were prepared and the complete microwave digestion procedure was applied to the reagent solutions.

For evaluating the accuracy of the method, two certified reference materials, MURST-ISS-A2 Antarctic Krill and CRM 063R Skim Milk Powder, were subjected to the same dissolution procedure and included in the overall analytical process.

Beverage Samples

A 25-mL aliquot each of wine, beer, and apple juice was treated with 5 mL of 65% (w/w) nitric acid and 5 mL of 30% (v/v) H_2O_2 in a beaker, placed on a programmable hot plate, and evaporated to near dryness. After this step, 10 mL of a solution of 70×10^{-3} mol L^{-1} tartaric acid was added and the procedure described above was followed.

TABLE III
Microwave Acid Digestion Program to Mineralize Food Samples

Sample weight	0.50 g	
Reagents	5 mL 65% (w/w) HNO_3 + 1.5 mL 30 % (v/v) H_2O_2	
	Final volume	25 mL

Microwave (Milestone) program:

Applied power (W)	Time (min)
250	1
0	1
250	5
400	5
600	5

Procedure

The acidified sample solutions containing the oxidant agent were merged at a Y-piece with the reductant and introduced into the hydride generator in a continuous flow system at 2.0 mL min^{-1} using a peristaltic pump. The PbH_4 generated was separated from the solution by means of a U-tube separator (GLS2) and swept by Ar (0.58 L min^{-1}) into the bottom of the quartz torch (the spray chamber was disconnected).

The lowest blanks were observed when tartaric acid was used to generate plumbane. The analytical signals obtained were the average of five replicate measurements. The effects of the interferents studied were calculated according to the following equation:

$$\% \text{ variation} = [(b-a) / b] \times 100$$

where a = Pb signal in the presence of interferent and b = Pb signal in the absence of interferent.

The analytical signals obtained were the average of five replicate measurements.

RESULTS AND DISCUSSION

Evaluation of Two Gas-liquid Separators (GLS1 and GLS2)

The experimental conditions used to evaluate the performance of both GLS separators are as follows: Pb concentration, 0.5 µg mL^{-1} and HNO_3 concentration, 0.2 mol L^{-1}. Lead is among the analytes that exhibits more difficulties when reduced to a hydride, and the chemical yield is rather low. For this reason, a strong oxidant and large amounts of reductant are necessary to improve sensitivity. In this study, different concentrations of $NaBH_4$ and $S_2O_8^{2-}$ were combined in order to achieve a fast, sensitive, and more efficient PbH_4 generation using both gas-liquid separators.

When the GLS1 was evaluated, the vigorous reaction (with pronounced aerosol formation) between the acidified sample with the added oxidant and the tetrahydroborate did not allow using concentrations of $NaBH_4$ and $S_2O_8^{2-}$ higher than 1.25 and 4%, respectively. As a consequence, the maximum Pb signal obtained under these conditions was around 25 (arbitrary units). To overcome this poor sensitivity, the use of a larger GLS with different characteristics was considered. The GLS2 was successfully used previously for the

determination of Ge by chloride generation coupled to ICP-OES (20). The reagents were conducted into the cell through 2.0-mm i.d. glass lines and the contact was only as thin films flowing down the interior walls of the central glass channel. This promoted intimate mixing, reduced excessive frothing due to hydrogen generation, and the process of phase separation is immediate through a thin liquid film phase only (19). A higher volume of the U-tube and a wider diameter drain tube was also beneficial to obtain smooth degassing of the waste solution while draining rapidly.

When the GLS2 was employed to generate plumbane, higher concentrations of $NaBH_4$ and $S_2O_8^{2-}$ could be used (2.5 and 6%, respectively), the system was more stable, and precision was improved. The sensitivity was 4-fold higher versus that obtained with the GLS1. It is important to note that even when it is desirable to minimize dead volume and reduce the level of sample consumption, a GLS with a higher volume was necessary for plumbane generation to improve sensitivity and precision due to the particular characteristics of this hydride.

Selection of Operating Conditions for Plumbane Generation

Chemical and physical parameters affecting the Pb hydride generation were optimized individually, while other parameters were fixed at their optimum value. Maximum signal-to-background ratio was always the optimization criterion. Unless otherwise noted, solutions containing 0.5 µg L^{-1} of Pb were used in the optimization process.

Chemical Parameters

Oxidant Concentration and Acidity Conditions

The effects of ammonium peroxidisulfate (persulfate) on the efficiency of Pb hydride generation were evaluated for each acid tested

(acetic, citric, nitric, and tartaric) at different concentrations. Acidity conditions and the acid selected to generate plumbane will depend on factors such as type and complexity of the matrix to be analyzed. In this study, nitric acid was evaluated because it is the most widely used reagent for plumbane generation. On the other hand, it was expected that chelating agents such as acetic, citric, and tartaric acid stabilize the metastable compounds that act as intermediate species in the formation of PbH_4; hence, these acids were tested.

Preliminary experiments demonstrated that when nitric acid was used as the reaction medium, higher blank values were obtained in comparison with those obtained with other acids; hence, nitric acid was distilled in a quartz sub-boiling still before use.

The interaction between persulfate and the acids tested on Pb signal is depicted in Figures 2–5. Persulfate concentrations were varied from 1–7% and a 2% (m/v) $NaBH_4$ solution was used as the reductant in all cases. The time necessary for pre-oxidation is critical. Under the experimental conditions of this study, maximum plumbane generation was obtained between 40 and 60 s after the addition of persulfate. Higher sensitivities were not obtained over 60 s. Oxidation of Pb markedly increased linearly with higher concentrations of persulfate in the four systems examined. Higher concentrations of oxidant than those observed in Figure 2 resulted in a violent reaction and the plasma was extinguished. In order to achieve good sensitivity with precision lower than 10%, the concentration of the oxidant chosen as the more convenient was 4% of acetic, citric, and tartaric acids), and 6% of nitric acid.

Reductant Concentration

The tetrahydroborate concentration presents a more marked effect

on the generation of Pb hydride in comparison with the other hydride-forming elements. The influence of $NaBH_4$ on plumbane generation from acetic, citric, nitric, and tartaric acids is shown in Figure 6. All solutions were stabilized in 0.1% (m/v) NaOH. The concentration of NaOH is critical because a sensitivity decrease was observed with higher concentrations. The flow rate of both acidified samples with oxidant and reductant were 1.5 mL min^{-1}. The best signal was achieved in citric and tartaric acids.

The concentration of tetrahydroborate is dependent on the system evaluated and, in all cases, plumbane production increased with reductant concentrations up to 3%. Above this value, higher concentrations of $NaBH_4$ produced a reaction so vigorous that the plasma extinguished. A compromise concentration of 2.5% (m/v) was selected as the more convenient in order to obtain more repeatability in the measurements.

Physical Parameters

Emission Line

The ratio I_{Pb}/I_b was calculated for four Pb(I) emission lines (nm): 220.353, 216.999, 261.418, and 283.306. The ratio I_{Pb}/I_b was: 3.05, 1.27, 0.83, and 0.67, respectively, for the four lines tested. The 220.353-nm wavelength was selected because it gave the best signal-to-background ratio.

Argon Carrier Flow Rate

The carrier gas affects the efficiency of transference and extraction of hydrides from the gas-liquid separator in the hydride generation system.

The Ar flow rate used to transport PbH_4 into the gas-liquid separator and then into the plasma torch was varied over the range of 0.58–0.90 mL min^{-1}. Figure 7 shows that the most suitable flow rate of Ar carrier gas in this system was
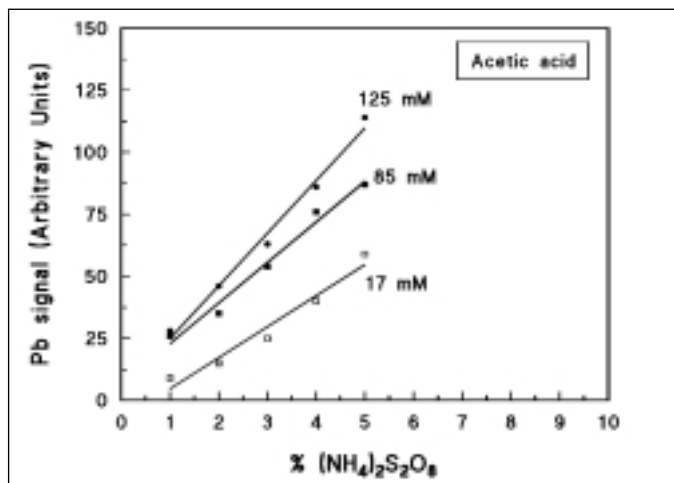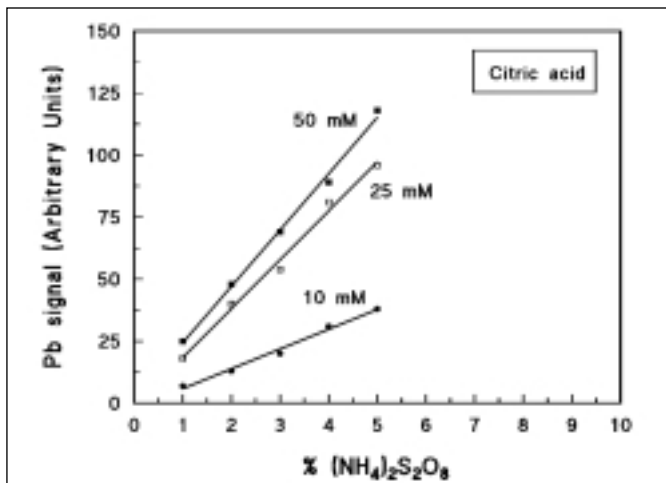
Fig. 2. Effect of persulfate concentration on Pb signal at different acetic acid concentrations. Pb, 0.5 M; NaBH₄ concentration, 2%; flow rate (sample and reductant), 1.5 mL min⁻¹; Ar flow rate, 0.75 L min⁻¹.
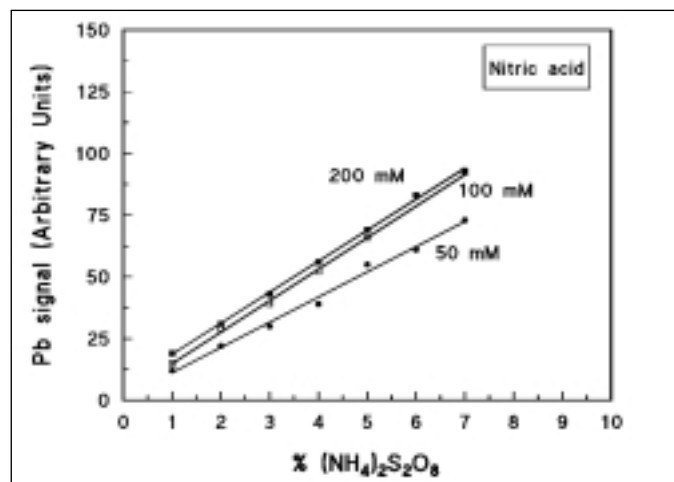

Fig. 3. Effect of persulfate concentration on Pb signal at different citric acid concentrations. Pb, 0.5 M; NaBH₄ concentration, 2%; flow rate (sample and reductant), 1.5 mL min⁻¹; Ar flow rate, 0.75 L min⁻¹.

Fig. 4. Effect of persulfate concentration on Pb signal at different nitric acid concentrations. Pb, 0.5 M; NaBH₄ concentration, 2%; flow rate (sample and reductant), 1.5 mL min⁻¹; Ar flow rate, 0.75 L min⁻¹.
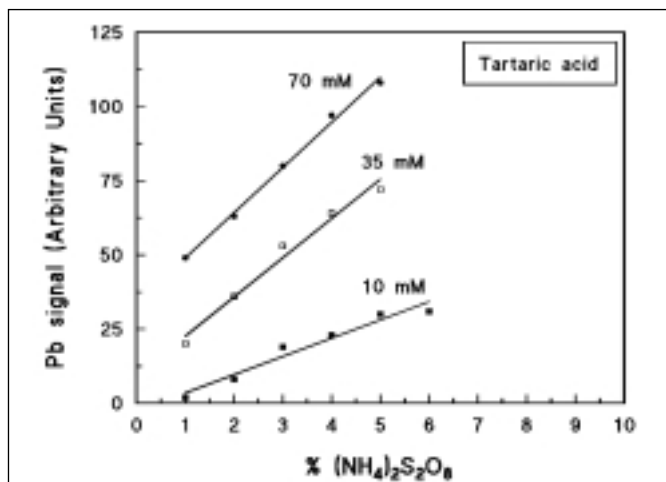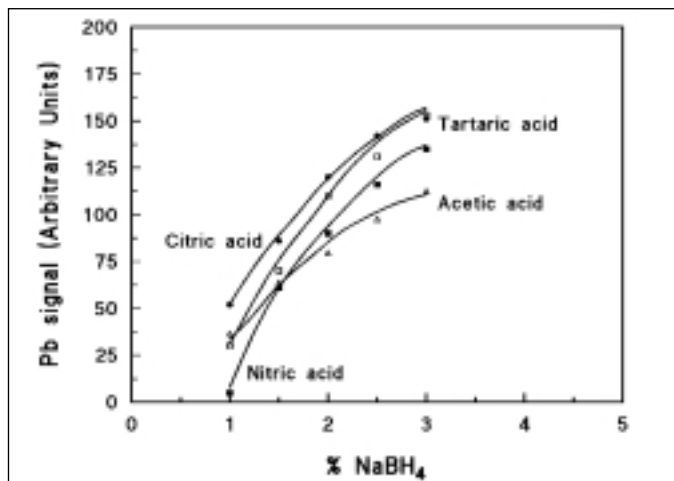

Fig. 5. Effect of persulfate concentration on Pb signal at different tartaric acid concentrations. Pb, 0.5 M; NaBH₄ concentration, 2%; flow rate (sample and reductant), 1.5 mL min⁻¹; Ar flow rate, 0.75 L min⁻¹.

0.58 L min⁻¹. Above this value, the Pb signal decreased steadily. The differences in sensitivity observed can be attributed to different excitation conditions experienced by the analyte when the Ar flow rate is changed.
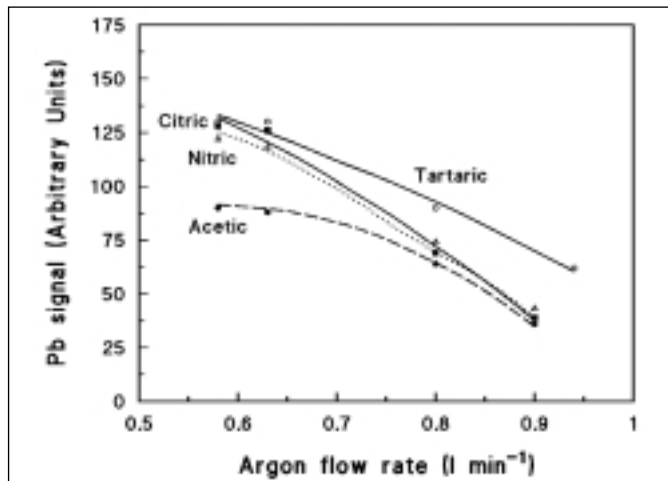
Reagent Flow Rate

To evaluate the effect of the pump speed, the acidified samples (containing the oxidant agent) and the reductant solutions were pumped (tube i.d. 1.1 mm) at flow rates ranging from 0.8–2.5 mL min⁻¹. The experimental data collected in Figure 8 show that PbH₄ production increases markedly with increasing reagent flow rates at least up to 2.5 mL min⁻¹.

The evolution of plumbane followed similar response profiles in the four systems studied. Reagent flow rates higher than 2.5 mL min⁻¹ produced vigorous hydrogen and resulted in extinguishing the plasma. When pump speeds higher than 2.0 mL min⁻¹ were tested, the repeatability of the measurements was poor and a precision higher than 10% was obtained. For this reason, a pump speed of 2.0 mL min⁻¹ was selected as the more convenient. However, if better detection limits are not required, lower flow rates can be used in order to reduce the reagent consumption. The conditions shown in Table I are recommended as optimal.

138

Fig. 6. Effect of NaBH₄ concentration on Pb signal in the four acids tested. Pb, 0.5 mg L⁻¹; flow rate (sample and reductant), 1.5 mL min⁻¹; 0.75 L min⁻¹; persulfate concentration, 4% (acetic, citric and tartaric acids) and 6% (nitric acid); Ar flow rate, 0.75 L min⁻¹.

Fig. 7. Influence of Ar carrier flow rate on Pb signal. Pb, 0.5 mg L⁻¹; NaBH₄, 2.5%; persulfate concentration, 4% (acetic, citric and tartaric acids) and 6% (nitric acid); flow rate (sample and reductant): 1.5 mL min⁻¹.
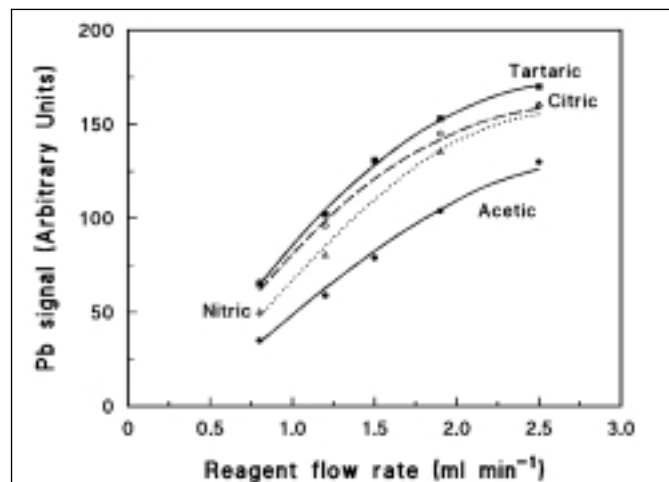
Fig. 8. Influence of reagents flow rate on Pb signal. Pb, 0.5 mg L⁻¹; NaBH₄, 2.5%; persulfate concentration, 4% (acetic, citric and tartaric acids) and 6% (nitric acid); Ar flow rate, 0.58 L min⁻¹.

Efficiency of Plumbane Generation

The efficiency of plumbane generation was calculated by quantifying the residual concentration of Pb in the waste of the hydride generator (GLS2). Measurements were performed by graphite furnace atomic absorption spectrometry (GFAAS) under the optimized conditions reported in the Instrumentation section. Solutions containing 0.5 and 1.0 μg mL⁻¹ Pb were used to calculate the efficiency of plumbane generation. The recoveries achieved were 85% (tartaric acid), 81% (citric acid), 77% (nitric acid), and 59% (acetic acid) for both concentrations.

Interference Study

The interference effects of elements such as Al, Cd, Co, Cr, Cu, Fe, Mn, Mo, Ni, V, and Zn on the generation of PbH₄ were studied because these elements compete with the analyte for reduction and catalyze NaBH₄ decomposition. Another group of typical interferents are volatile hydride elements (Periodic group IV A, V A, and VI A). For this reason, the effects of As, Bi, Ge, Sb, Se, Sn, and Te on the Pb signal were evaluated. The effect of Hg on PbH₄ evolution was also observed. In the particular case of lead, the effect of foreign ions can be different in the presence of an oxidizing agent and the mechanisms involved can also be different.

Interference studies in all the reaction media at the optimized working conditions and at the optimal concentration of the acids were investigated. Variations over ±5% in the analytical signal of Pb in the presence of other elements were taken as an interference. All samples analyzed contained 0.5 μg L⁻¹ of Pb and the results are the averages of five measurements. Blank solutions were analyzed for each matrix and matrix plus potential interfering ion. The results of the interference study are summarized in Tables IV and V. Enhancing effects were not observed. Selenium and tellurium are the hydride-forming elements that more severely affect plumbane generation in the four systems tested. However, the effect of Se(IV) was less pronounced in tartaric acid.

When the effect of transition metals was evaluated, it is evident from Table V that Ni is a serious depressive interference in the majority of the acids tested to the extent that the Pb signal is completely inhibited in

TABLE IV
Interferences of Hydride-forming Elements and Hg in the Determination of Pb by HG-ICP-OES in Acid Media
Results given are % change in lead signal (Pb: 0.5 mg L^{-1}, NaBH$_4$: 2.5%).

Ion	Interferent mg L^{-1}	Tartaric 70 mM	Citric 50 mM	Nitric 200 mM	Acetic 125 mM
Sb(III)	50	−10	−12	−77	−67
Sn(IV)	50	0	a	−70	a
Se(IV)	50	−59	−95	−96	−92
As(III)	50	0	0	0	0
Bi(III)	50	−19	−42	−100	−40
Te(IV)	50	−41	−89	−97	−85
Ge(IV)	50	0	a	0	a
Hg(II)	50	0	−14	−39	a

a Not measurable because of instability of the system (high H$_2$ evolution and the plasma extinguishes).

TABLE V
Interferences of Heavy Metals in the Determination of Pb by HG-ICP-OES in the Acid Media
Results given are % change in lead signal (Pb: 0.5 mg L^{-1}, NaBH$_4$: 2.5%).

Ion	Interferent mg L^{-1}	Tartaric 70 mM	Citric 50 mM	Nitric 200 mM	Acetic 125 mM
Cr(III)	50	0	0	0	0
Mn(II)	50	0	0	0	0
Co(II)	50	−26	−55	−62	−73
Cd(II)	50	−45	−87	−92	−67
Cu(II)	50	−44	−92	−89	−80
Zn(II)	50	-67	−87	−86	−79
Ni(II)	50	−100	−87	−100	−94
V(V)	50	0	0	0	0
Al(III)	50	0	0	0	0
Mo(VI)	50	−41	−79	−74	−87
Fe(III)	50	−19	0	0	a

a Not measurable because of instability of the system (high H$_2$ evolution and the plasma extinguishes).

tartaric and citric acids. Cr(III), Mn(II), V(V), and Al(III) are the only species tolerated by the acids evaluated without any adverse effects on the Pb signal.

Discrepancies about the effect exerted on the Pb signal by diverse elements are generally observed in the literature. It can be explained by the different generation devices, instrumentation, and analytical conditions (medium, oxidizing agent)

employed. In spite of this, there is general consensus that Pb is vulnerable to depressive interferences.

The study of the influence of foreign ions on plumbane generation showed that, even when not completely eliminated, tartaric acid exerted better control of interferences in comparison with the other acids tested.

Quality Parameters

The acids studied were also compared in terms of their analytical performance as a preliminary step to the determination of Pb in food and beverage samples by HG-ICP-OES.

The detection limits were calculated following the IUPAC rules on the basis of the 3 σ criterion for 10 replicate measurements of the blank signal and the results averaged between 4.4 and 6.8 μg L^{-1} (Table VI) depending on the acid evaluated. Precision was evaluated for the four reaction media studied using a standard containing 0.5 μg L^{-1} of Pb and the (%) RSD values obtained were in the range 5.4 to 6.7 for 10 replicate measurements. The results are shown in Table VI. The characteristic masses of the analytical method were evaluated and ranged from 0.6 to 1.1 ng depending on the sample analyzed.

Compared with conventional continuous nebulization (CN), the coupling of HG-ICP-OES results in a sensitivity increase of a factor of approximately two orders of magnitude. In all cases, the linear calibration curves ranged approximately four orders of magnitude. Accuracy tests for the entire analytical procedure were performed by means of the analysis of two certified reference materials, MURST ISS-2 Antarctic Krill and CRM 063R Skim Milk Powder. The results are listed in Table VII.

Analysis of Real Samples

From the study performed, tartaric acid can be considered the best alternative to determine low levels of Pb in freeze-dried food samples and different kinds of beverages. This is based on the fact that a better control of interferences was observed.

Predigestion of solid samples was necessary prior to the microwave dissolution to allow

TABLE VI
Analytical Performance for
Pb Determination as PbH$_4$

Acid	Detection Limit (3 σ)[a] (ng mL^{-1})	Precision (%)[a] (for 0.5 μg L^{-1} Pb)
Acetic	6.8	5.9
Citric	4.9	6.1
Nitric	5.4	6.7
Tartaric	4.4	5.4

[a] (n = 10).

a more efficient attack of the samples. As with biological media (in the analysis of wines and soft drinks), it is necessary to take into account bonds between Pb and the organic groups. Liquid samples were also subjected to a preliminary oxidation process as described in the Sample Preparation section.

Lead was determined in three independent aliquots of each sample and calibration was achieved in all cases by the standard addition method because when Pb was determined by interpolation of the calibration curve, lower recoveries were obtained. The results obtained are presented in Table VIII.

TABLE VII
Evaluation of Method Accuracy
Lead Concentrations Expressed in μg g^{-1} (mean concentration ± S. D.)

Reference Material	Certified	Found
MURST-ISS-A2 Antarctic Krill	1.11±0.11	0.98±0.08
CRM 063R Skim Milk Powder	18.5±2.7	20.1±1.3

TABLE VIII
Lead Content of Selected Foods and Beverages (n=3)

Sample	Lead Content
Apple juice (commercial)	26.3±1.2 μg L^{-1}
Red wine (Pinot noire)	65.9±2.2 μg L^{-1}
Table wine (red)	44.1±1.9 μg L^{-1}
Table wine (white)	76.1±3.6 μg L^{-1}
White beer	115±5 μg L^{-1}
Dark beer	101±5 μg L^{-1}
Potato	< LOD
Egg	0.93±0.06 μg g^{-1}
Tomato	9.21±0.45 μg g^{-1}
White bread	5.33±0.29 μg g^{-1}
Skim milk powder	2.01±0.11 μg g^{-1}
Cereal food	< LOD
Mussel	2.12±0.10 μg g^{-1}
Cuttlefish	1.90±0.09 μg g^{-1}

CONCLUSION

This work is an attempt to improve the efficiency of lead hydride generation by modifying the acid medium. However, the results obtained using organic acids only represented a slight improvement (even with tartaric acid). Nevertheless, a noticeable control of interferences was achieved with tartaric acid which also improved the sensitivity of the method. In addition, the high efficiency of plumbane generation (85%), obtained with the proposed method, confirms that the presence of a chelating agent such tartaric acid is beneficial to stabilize the intermediate Pb(IV) metastable compounds, thus improving the kinetics of the reaction.

Received January 29, 2003.

REFERENCES

1. U. Ewers and H-W Schlipköter, in "Metal and their compounds in the environment," Ernest Merian, (ed), VCH, Germany (1991).

2. I. Aroza, M. Bonilla, Y. Madrid, and C. Cámara, J. Anal. At. Spectrom. 4, 163 (1989).

3. J. Sanz, P. Basterra, J. Galbán, and J. R. Castillo, Mikrochim. Acta 1, 271 (1989).

4. Y, Madrid, M. Bonilla, and C. Cámara, Analyst 115, 563 (1990).

5. I. D. Brindle and X. Le, Anal. Chem. 61, 1175 (1989).

6. M. C. Valdés-Hevia y Temprano, M. R. Fernández de la Campa, and A. Sanz-Medel, J. Anal. At. Spectrom. 8, 821 (1993).

7. D. L. Tsalev, P. B. Mandjukov, and D. L. Draganova, Spectrosc. Lett. 25, 943 (1992).

8. H. D. Fleming and R. G. Ide, Anal. Chim. Acta 83, 67 (1976).

9. J. R. Castillo, J. M. Mir, C. Martínez, and J. Val, P. Colón, Mikrochim. Acta 1, 253 (1985).

10. Y. Madrid, J. Meseguer, M. Bonilla, and C. Cámara, Anal. Chim. Acta 237, 181 (1990).

11. P. N. Vijan and G. R. Wood, Analyst 101, 966 (1976).

12. K. Jin, M. Taga, H. Yoshida, and S. Hikime, Bunseki Kagaku 27, 759 (1978).

13. K. Jin and M. Taga, Anal. Chim. Acta 143, 229 (1982).

14. Y. Madrid, M. Bonilla, and C. Cámara, J. Anal. At. Spectrom. 4, 167 (1989).

15. C. Nerin, S. Olavide, and J. Cacho, Anal. Chem. 59, 1918 (1987).

16. J. Aznarez, F. Palacios, J. C. Vidal, and J. Galbán, Analyst 109, 713 (1984).

17. M.C. Valdés-Hevia y Temprano, B. Aizpún Fernández, and M.R. Fernández de la Campa, Anal. Chim. Acta 283, 175 (1993).

18. Y. Madrid and C. Cámara, Analyst 119, 1647 (1994).

19. R.E. Sturgeon, J. Liu, V.J. Boyko, and V.T. Luong, Anal. Chem. 68, 1883 (1996).

20. S. Farías and P. Smichowski, J. Anal. At. Spectrom. 14, 809 (1999).

Multichannel Vapor Phase Digestion (MCVPD) of High Purity Quartz Powder and the Determination of Trace Impurities by ICP-AES and ICP-MS

K. Dash, S. Thangavel, S.M. Dhavile, K. Chandrasekaran, and *S.C. Chaurasia
National Centre for Compositional Characterisation of Materials
Bhabha Atomic Research Centre
ECIL (Post), Hyderabad - 500 062, India

INTRODUCTION

High purity quartz is widely applied in optical wave-guide fiber, semiconductor, and photovoltaic materials. The relevant desirable properties of quartz used in high technology industries are seriously affected by trace metal impurities (1). Moreover, trace elements also influence the electro-optical properties of quartz, which are important in other applications. Quartz matrix is usually dissolved for trace analysis with the aid of HF (2,3) or HF / mannitol (4), followed by subsequent volatilization of SiF_4.

These reagents are often contaminated with traces of foreign elements and a dissolution procedure requires quantities of acid (HF) in excess of 10 times (2,3) the sample weight, which results in unacceptable reagent blank values. Additionally, to exploit the full advantage of the sensitivity and accuracy of the ICP-MS/ICP-AES techniques, the process/reagent blank should be held to no more than a few percent of the amount being determined. One method of achieving low reagent blank values is the separate purification of hydrofluoric acid by sub-boiling distillation followed by conventional dissolution. There are numerous difficulties in handling and storing high purity acids once they have been prepared (5). High purity HF available from commercial sources is satisfactory for many trace element determinations, but is not always adequate for ultra-trace level determination either due

*Corresponding author.
e-mail: scc@cccm1.ernet.in
Fax: (040)7125463

ABSTRACT

A simple method is described for *in situ* reagent purification in a multichannel vapor phase digestion (MCVPD) system with simultaneous dissolution of high purity quartz samples. This MCVPD procedure has two major advantages: namely, significant reduction (20–1000 times) in process blank values of trace metals from impure or GR/AR grade HF and 21 samples can be digested at a time. Metallic trace impurities in high purity quartz samples were determined by ICP-AES and ICP-MS. The achievable detection limits (3 σ) were between 0.6 ng g^{-1} (Li, Cd) and 50 ng g^{-1} (K). The accuracy of the results was checked by their comparison with those obtained by conventional dissolution with Suprapur grade HF. Through use of this MCVPD procedure, GR/AR grade HF can be used in place of expensive highly pure-grade HF for trace metal determination in a quartz matrix.

to a lack of purity or high upper specification limits.

In view of the problems associated with the preparation and storage of highly pure HF, the ultimate approach of silica matrix dissolution, while preventing the introduction of impurities, is by vapor phase decomposition (VPD) (3) instead of conventional HF dissolution. A VPD procedure for trace element determination in high purity quartz at 180ºC in a sealed PTFE bomb (6) and phosphorus by ICP-MS after VPD at an elevated pressure (7) has been reported. Control of temperature and pressure inside such pres-

surized vessels requires special sensors, the lack of which could result in safety problems. In most of the reported vapor phase digestion procedures (6–8), only 1–2 samples can be digested within a time period of 8–12 hours. Thus, the determination of trace impurities in a large number of high purity quartz samples on a routine basis using VPD is a time-consuming task.

In the described vapor phase digestion procedure, a polypropylene vessel has been used in which a large number of high purity quartz samples (16–18 samples and 3–5 blanks, respectively) are digested at a time. Performance of this MCVPD procedure for *in situ* reagent purification and multiplex sample digestion is demonstrated by the determination of 17 trace elements in high purity quartz using ICP-MS and ICP-AES.

EXPERIMENTAL

Instrumentation

Elemental analyses were performed by ICP-MS and ICP-AES. A Model VG PlasmaQuad PQ3 (VG Elemental, UK) ICP-MS instrument was used with the operating conditions summarized in Table I. Sample introduction was effected by pneumatic nebulization using a Meinhard® concentric nebulizer, a double-pass Scott-type spray chamber cooled to 4ºC using a Neslab recirculating chiller and a Fassel type torch. The ICP-MS conditions were optimized for maximum sensitivity using a 10-ng/mL tuning solution of Be, Co, In, and Bi in 2% HNO_3. Rhodium was used as an internal standard for all samples.

TABLE I
Instrumental Parameters

ICP-MS Instrument	VG PlasmaQuad PQ3
Power	1350 W
Nebulizer gas flow	0.75 L/min
Auxiliary gas flow	0.81 L/min
Plasma gas flow	13.1 L/min
Spray chamber temp.	4ºC
Nebulizer	Meinhard concentric nebulizer
Sample Cone, Ni	1.0 mm
Skimmer Cone, Ni	0.7 mm
Detector Mode	Dual mode (PC/analog)
ICP-AES Instrument	Sequential spectrometer, JY 2000 (Jobin Yvon, Horiba, France)
Generator	900 W at 40.6 MHz
Monochromator	0.64 m, 2400 lines/mm, Czerny Turner mounting
Plasma gas	13 L/min
Aerosol carrier gas	1.2 L/min
Nebulizer	Concentric nebulizer with cyclonic spray chamber

Fig. 1. MCVPD assembly. All dimensions are in mm.

A Model JY-2000 ICP-AES (Jobin Yvon, Horiba group) sequential spectrophotometer was used with the operating parameters also listed in Table I. All determinations were carried out using external calibration.

Reagents and Standards

Suprapur® grade (E. Merck, Darmstadt, Germany) HF 40%, HNO_3 (65%), and H_2SO_4 (96%) as well as respective GR grade acids were used. Pure grade HF (40%) was obtained from Merck, India. High purity deionized water (18 $m\Omega \cdot cm$) was prepared using a Milli-Q™ water purification system (Millipore, Bedford, MA, USA). After preparation, all reagents were stored in cleaned PFA bottles. Single-element standards of Li, Al, Ca, V, Cd, Co, Cr, Cu, Fe, K, Mg, Mn, Mo, Na, Ni, Ti, and Zn (E. Merck) were used to prepare the multielement calibration standards. Working standard solutions were prepared by diluting the multielement stock standard solutions with 2% Suprapur HNO_3, when required.

MCVPD of quartz powder samples was carried out in 5-L capacity polypropylene vessels. A perforated sample rack (~ 218 mm i.d., 10 mm thickness) made out of polypropylene sheet was placed inside the polypropylene vessels. Twenty-one grooves (i.d. 31 mm x depth 8 mm) were machined on the sample rack in which the sample containers were stored. Fifty-seven holes (i.d. 10 mm) were drilled to channel the acid vapors into the sample compartment. The polypropylene vessels and lids were air-locked. To ensure that the vessels were completely leak-proof, they were covered with a 0.2-mm thick circular (i.d. 260 mm) Teflon® sheet with the lids pressed into the vessels. The complete MCVPD assembly is shown in Figure 1 with detailed dimensions. The PFA vials (Cole Parmer, 22-mL
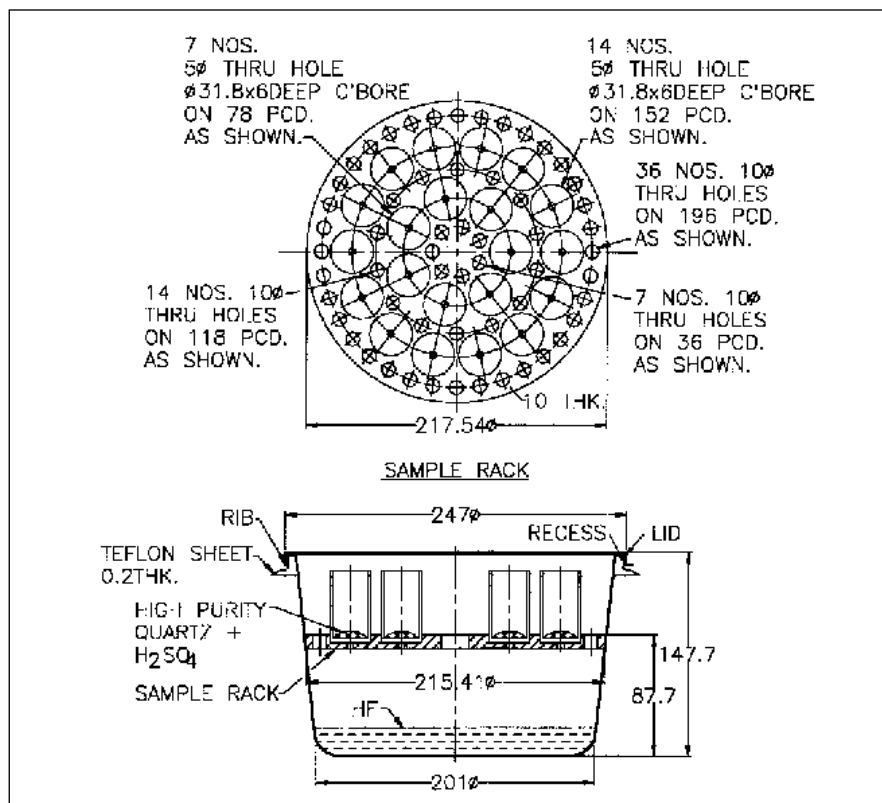
capacity, 29-mm i.d., with 52 mm in height) were used as sample containers.

Labware

All necessary precautions were taken to minimize contamination during all phases of the analysis because of the low concentration of the elements being determined. All labware was cleaned thoroughly by leaching in hot (1:1) HNO_3 and then rinsing with ultrapure water. To clean the MCVPD apparatus, a mixture of HF and HNO_3 (1:1) was put in the bottom of the reagent compartment. After capping the lid along with the Teflon® sheet, the inside of the apparatus was leached over a water bath for one hour. After cooling, it was thoroughly rinsed with Milli-Q™ water and always kept in closed condition when not in use. After one capping, the Teflon sheet remained attached to the lid. Before capping the vessel for VPD, the Teflon sheet surface was thoroughly washed with Milli-Q water using a fine spray from a spray bottle.

Sample Decomposition

After cleaning the MCVPD apparatus (as described before), the unit was assembled in a laminar flow clean bench. The quartz samples (mesh size 50–100) of 1 g were weighed into the PFA vials in a Class 1000 clean room and 200 μL of H_2SO_4 was added to each quartz sample. The PFA vials were then placed in the grooves (31 mm i.d.) of the sample rack. 250 mL of pure/GR grade HF was carefully poured into the reagent reservoir using a polypropylene funnel. The vessels were capped, transferred to a fume hood, and placed on a single-hole (180-mm i.d.) water bath for digestion. An exposure of eight hours was required for complete digestion of 16 quartz samples (16 x 1 g, 5 blanks). When the dissolution was complete, the MCVPD assembly was allowed to cool to room temperature. The PFA vials were then removed from the sample rack with a forcep, capped, and dried externally. The PFA vials were then heated at approximately 100°C on a ceramic top hot plate in a laminar flow clean bench (Class 10), until a residue of 200 μL, containing all impurities associated with the sample, remained. After evaporation of silicon tetrafluoride, the trace residues were made up to 10-mL volume with 2% HNO_3 using an Eppendorf micro pippete (5-mL capacity). These diluted solutions were introduced into the ICP-MS and ICP-AES for trace metal determination.

RESULTS AND DISCUSSION

Advantages of MCVPD

A simple and inexpensive polypropylene vessel was employed as the reaction chamber for MCVPD to avoid the use of a more expensive chamber, machined from a solid block of Teflon (7). The polypropylene vessel used in this MCVPD experiment was partitioned into a reagent compartment (lower portion) and a sample compartment (upper portion) by placing a perforated sample rack in between (Figure 1). On heating the assembly, vapors of HF from the reagent compartment are channeled into the sample compartment which dissolve the samples. Thus, trace impurities in the liquid reagent are not added to the sample and allows for *in situ* reagent purification. Additionally, the PFA sample vials are situated at a height of 80 mm above the impure reagent, i.e., HF. This large separation in height between the sample and liquid HF ensures that contamination of impure reagents (HF) is completely eliminated. This digestion assembly does not involve high temperature and pressure and thus avoids the use of expensive ancillary devices for temperature / pressure control. The major constraint in the VPD

procedures reported for routine analysis is that only 1–2 samples can be digested at a time (6–8). In this respect, the unique feature of this MCVPD is high sample throughput. In a single batch, 16–18 quartz samples along with 5–3 blanks, respectively, can be digested. For 16 quartz samples (16 x 1 g), the optimum dissolution time was found to be eight hours [250 mL of HF (40–48%)]. Simultaneous digestion of multiple samples greatly increases the sample throughput in spite of the slow dissolution rate under conventional heating.

Evaluation of Purification by MCVPD

To evaluate the extent of purification by the described procedure, GR and pure grade HF (250 mL) was taken in the reagent compartment and VPD was carried out. Process blank values by conventional and corresponding MCVPD dissolution for various trace impurities were determined and are presented in Table II. No statistically significant differences were observed in the MCVPD process blanks for trace metal impurities, when the VPD was carried out using these two different grades of acids with large differences in trace impurity concentrations. This implies that impurities in both pure and GR grade HF do not contaminate the sample. In other words, *in situ* purification was achieved during MCVPD of the quartz samples. Process blank values between conventional (with pure grade HF) and corresponding process blank values obtained by MCVPD demonstrate the *in situ* purification efficiency of the MCVPD apparatus (Table II). The process blank of Fe, which was 1200 ng/mL in pure grade HF (conventional dissolution), was reduced to 6 ng/mL, a purification factor of 200. Another example is Na, which was reduced to 7 ng/mL from 2000 ng/mL, with a purification factor of

285. The vanadium content was reduced to 0.1 ng/mL from 100 ng/mL, and a purification factor of 1000 was achieved. It is also evident from Table II that by using cleaner HF, i.e., GR grade HF, there was no improvement of blank levels in the MCVPD process. Additionally, the phosphorus reagent blank was reduced 450 times through this MCVPD process and phosphorus was determined by a spectrophotometric method (9).

Comparison of MCVPD Process Blank With that of Suprapur HF

Suprapur grade HF (10 mL) and 200 µL of Suprapur H_2SO_4 were taken in PFA vials and evaporated on the hot plate in the laminar flow clean bench (Class 10). After evaporation of all HF, the content was made up to 10 mL volume with 2% Suprapur HNO_3. Process blank values of trace elements thus obtained (Suprapur HF) are compared against the MCVPD process blank in Table II. The data in Table II show that MCVPD process blanks were very low and independent of the impurity concentrations in the HF used for vapor phase digestion. These process blank values were comparable or superior in many cases to the Suprapur grade HF process blank. In fact, the blank values for Na, Ca, and K from Suprapur grade HF were double that of the MCVPD process blank. The Ni process blank is nearly five times less than that of Suprapur HF blank.

Cross-contamination and Recovery Study

In the MCVPD vessel, 16–18 quartz samples and 5–3 blanks were digested. Cross-contamination of analytes between sample to sample or sample to blank can result in unreliable blank values and thus would affect the precision and detection limit as well. To establish that no cross-contamination occurred, two sets of experiments were carried out. In the first set, five blanks were digested (without sample in the rest of the 16 PFA vials, as described in the Procedure section, and the trace element concentrations of critical elements (Na, Ca, Al, etc.) determined. In the second set, a pre-analyzed quartz sample (1 g) was taken in each of the 16 PFA vials. The MCVPD was carried out for five process blanks in the presence of 16 quartz samples. Then the process blank values for critical trace elements (Na, Al, etc.) were determined and the results are presented in Table III. It was found that the process blank levels of trace impurities were the same in the presence or absence of 16 quartz samples during the MCVPD process. For example, a process blank of 5 ng/mL was obtained for Al, when the sample contained 4500 ppb of Al. This process blank of 4–5 ng /mL for Al was also obtained during the MCVPD procedure in the absence of sample. Similarly, MCVPD process blanks were obtained for other critical elements such as Ca and Na, when the blanks were digested along with sample. These observations established the absence of any cross-contamination.

TABLE II
Comparison of Process Blank Values Using Various Grades of HF by Conventional and Corresponding MCVPD Dissolution for 1 g of Quartz Powder (ng/g)

Element	Conventional[a] Pure grade	MCVPD[b] Pure grade	Conventional[a] GR grade	MCVPD[b] . GR grade	Conventional[c] HF Suprapur grade
Na	20,000	60 ± 12	640	70 ± 13	120 ± 16
K	15,000	60 ± 16	280	60 ± 16	90 ± 20
Ca	5000	45 ± 8	800	50 ± 9	100 ± 13
Ti	800	40 ± 10	260	40 ± 8	40 ± 10
Fe	12,000	60 ± 10	680	70 ± 12	70 ± 12
^{7}Li	40	1.5 ± 0.2	5	1.5 ± 0.4	1.0 ± 0.2
^{24}Mg	1200	13 ± 2.3	360	12 ± 2.5	10 ± 3
^{27}Al	1600	50 ± 3	300	40 ± 2.5	30 ± 11
^{51}V	1000	1.0 ± 0.2	4	0.9 ± 0.2	2.0 ± 0.4
^{52}Cr	80	7 ± 0.6	30	6 ± 0.5	8.2 ± 1.1
^{55}Mn	400	6 ± 0.3	220	7 ± 0.5	7.4 ± 0.3
^{59}Co	20	0.5 ± 0.2	7	0.7 ± 0.3	0.9 ± 0.2
^{58}Ni	300	3.8 ± 0.8	50	3.3 ± 0.8	15 ± 1.5
^{63}Cu	1500	3 ± 1.2	16	4 ± 1.4	2.3 ± 0.3
^{66}Zn	1000	6 ± 1.5	140	5 ± 1.4	9.6 ± 2.3
^{98}Mo	160	4 ± 0.3	12	2 ± 0.2	3.0 ± 0.4
^{111}Cd	10	0.4 ± 0.2	3.8	0.8 ± 0.3	0.4 ± 0.1

Na (588.99 nm), K (766.49 nm), Ca (393.36 m), Fe (238.20 nm), and Ti (334.94 nm) were determined by ICP-AES and the remaining elements by ICP-MS.

[a] Process blank (n=2) in conventional dissolution obtained by evaporating 10 mL of HF (GR or pure grade) in the presence of 200 µL of Suprapur H_2SO_4 and then made up to 10-mL volume with 2% HNO_3.

[b] The concentration of the MCVPD process blank (n=5) is the elemental concentration of the reagent blanks that were diluted with 2% HNO_3 (10 mL) after being processed through the MCVPD procedure.

[c] Process blank for Suprapur grade HF was obtained by evaporating 10 mL of HF in the presence of 200 µL Suprapur H_2SO_4 and finally made up to 10-mL volume with 2% of HNO_3.

Recovery behavior of the analytes during vapor phase digestion was studied by spiking quartz samples with elements of interest. The recovery of spikes was between 97–102%.

Analysis of Samples and Detection Limits

In the vapor phase dissolution method described, boron is completely lost, as sulfuric acid chars mannitol and thus precludes the use of this complexing agent. The detection limits given in Table IV are 3 σ values based on MCVPD process blanks (n=5). Detection limits are, with the exception of K and Na, in the 0.5 to 30 ng g^{-1} range. Due to mass interference from $^{40}Ar^{16}O^+$, the determination of ^{56}Fe (most abundant isotope) was not possible by ICP-MS. Further, ^{57}Fe suffers from interference due to $^{40}Ar^{16}O^1H^+$ (10). Similarly, the most abundant isotope of titanium (^{48}Ti, 73.7%) is interfered by $^{32}S^{16}O^+$ ions due to the presence of residual sulfuric acid in the medium. This is difficult to correct by means of blank subtraction as the concentration of residual H_2SO_4 is variable. When the other isotope of Ti, i.e., ^{47}Ti having natural abundance of 7.5%, was used, it produced high detection limits (~300 ng/g). Therefore, Fe and Ti were determined by ICP-AES. The results for the two highly pure quartz samples are given in Table IV together with the results obtained by conventional dissolution (2) using highly pure grade HF. The standard deviation was deduced from five measurements of the sample. The results using the MCVPD procedure agreed reasonably well with the established method of conventional dissolution. The precision of the method, expressed as the relative standard deviation of five independent analyses of the sample, provided RSD values of less than 8% for most of the analytes.

TABLE III
**MCVPD Process Blank[a] Values for Critical Trace Elements
(Na, Al, and Ca) in Presence and Absence of Samples (ng/mL) [b]**

Elements	Blanks Without Sample	Blanks With Sample
Na	6.0 ±1.2	5.0 ±1.3
Al	4.0 ±1.2	5.0 ±1.0
Ca	5.0 ± 0.8	4.5 ±0.7

[a] The concentration of the MCVPD process blank (n=5) is the elemental concentration of the reagent blanks that were diluted with 2% HNO$_3$ (10 mL) after being processed through the MCVPD procedure.
[b] Mean ± Standard Deviation (n=5).

TABLE IV
**Trace Element Concentrations Determined by ICP-AES and ICP-MS
After MCVPD and Conventional HF (Suprapur Grade) Dissolution
(ng/g) [a]**

Element	Det. Limit (MCVPD)	High Purity Quartz-I		High Purity Quartz II	
		MCVPD	Conventional Dissolution[b]	MCVPD	Conventional Dissolution[b]
Na	36	600 ± 44	615 ± 50	1800 ± 170	2050 ± 260
K	50	750 ± 78	810 ± 80	1120 ± 130	1180 ± 140
Ca	25	200 ± 15	195 ± 15	480 ± 31	510 ± 38
Ti	30	2100 ± 150	2080 ± 150	3580 ± 260	3450 ± 250
Fe	33	260 ± 23	285 ± 25	490 ± 35	550 ± 44
^7Li	0.6	20 ± 1	20 ± 2	60 ± 4	58 ± 4
^{24}Mg	7	36 ± 3	38 ± 2	65 ± 4	62 ± 5
^{27}Al	10	4520 ± 325	4350 ± 330	6680 ± 475	6900 ± 400
^{51}V	0.5	11 ± 1	13 ± 2	12 ± 2	10 ± 1
^{52}Cr	2	60 ± 4	65 ± 3	50 ± 4	47 ± 3
^{55}Mn	0.8	26 ± 3	27 ± 4	75 ± 7	85 ± 9
^{59}Co	0.7	11 ± 1	12 ± 1	28 ± 3	31 ± 3
^{58}Ni	2.5	36 ± 5	34 ± 5	60 ± 4	59 ± 3
^{63}Cu	3.6	35 ± 4	36 ± 4	150 ± 11	140 ± 12
^{66}Zn	4.5	25 ± 4	27 ± 5	18 ± 3	21 ± 4
^{98}Mo	0.9	< 3	< 3	< 3	< 3
^{111}Cd	0.6	< 2	< 2	< 2	< 2

[a] Mean ± Standard Deviation (n=5).
Na (588.99 nm), K (766.49 nm), Ca (393.36 nm), Fe (238.20 nm,) and Ti (334.94 nm) were determined by ICP-AES and the remaining elements by ICP-MS.
[b] In conventional dissolution, 1 g of SiO$_2$ was dissolved in 10 mL of HF (Suprapur grade) with 200 μL of H$_2$SO$_4$ and, after evaporation of silicon-related matrix, was made up to 10-mL volume with 2% nitric acid.

CONCLUSION

The main advantages of using the MCVPD process are simplicity and low cost of AR/GR/pure grade hydrofluoric acid used in place of expensive, highly pure grade HF; and more importantly, multiple numbers of samples can be digested in a single batch. Additionally, the whole MCVPD assembly requires only a polypropylene vessel, where a perforated sample rack has to be fabricated. Most of all, these cost saving measures do not compromise the quality of the analytical results.

REFERENCES

1. J.W. Mitchell, Pure Appl. Chem. 54, 819 (1982).

2. R.Bock, A Handbook of decomposition methods in Analytical Chemistry, International Textbook Company, Glasgow, UK (1979).

3. Morris Zief and James W.Mitchell, Contamination control in trace element analysis, John Wiley & Sons, New York (1976).

4. D.Karunasagar, K.Dash, K.Chandrasekharan, and J.Arunachalam, At. Spectrosc. 21(6), 216, (2000).

5. J.R.Mody and E.S. Beary, Talanta 29, 1003 (1982).

6. Isao Kojima, Fumihiko Jinno, Yasuhiko Noda, and Chuzo Lida, Anal. Chim. Acta 245, 35 (1991).

7. K.Fujimotto, M.Ito, M.Shimura, and K.Yoshiko, Buneski Kagaku 47/3, 187 (1988).

8. J.F.Wooley, Analyst 100, 896 (1975).

9. S.Thangavel, K.Dash, and S.C. Chaurasia, Talanta 55, 501 (2001).

10. Akbar Montaser, Inductively Coupled Plasma Mass Spectrometry, Wiley-VCH (1998).

Cation Exchange Chromatographic Group Separation and ICP-AES Determination of Rare Earth Elements and Yttrium in Refractory Minerals Zircon, Ilmenite, Rutile, Columbite-Tantalite, Garnet, and Silliminite

*A. Premadas
Chemical Laboratory, Atomic Minerals Directorate for Exploration and Research
Civil Lines, Nagpur, India - 440001

ABSTRACT

A simple cation exchange chromatographic group separation is described for the inductively coupled plasma atomic emission spectrometric (ICP-AES) determination of rare earth elements and yttrium in refractory minerals such as zircon, ilmenite, rutile, columbite-tantalite, garnet, and silliminite. The method described is very effective for the quantitative removal of milligram amounts of zirconium, titanium, niobium, and tantalum from microgram amounts of REEs and Y. Complete removal of zirconium is not possible using either oxalate or fluoride precipitation separation. The zircon, ilmenite, and rutile samples were fused with a flux (powdered mixture of 3:1 ratio of potassium bi fluoride and sodium fluoride), and the cooled melt was treated with sulphuric acid for the removal of fluoride. The contents were taken in ~ 0.25 M oxalic acid solution. The acidity of the solution was maintained around 1 N, in ~150-mL volume, and used for the cation exchange group separation of REEs and Y.

The columbite-tantalite samples were fused with potassium bi-sulphate and the solution was prepared in oxalic acid for the ion exchange separation of REEs. Samples like garnet and silliminite minerals were treated with acid digestion using hydrofluoric, hydrochloric, and perchloric acids, and the residue (undissolved material) was fused with the flux, treated with sulphuric acid as above, and taken in water. The combined solution was used for the ion exchange separation.

The conditions for the cation exchange separation of REEs and Y in these types of minerals were optimized based on the presence of oxalic acid, salts derived by fusion of the refractory minerals using the flux, and concentration of sulphuric acid used for the decomposition of the samples.

Spectral interference studies of milligram quantities of Zr, Ti, Nb, and Ta on the ICP-AES determination of micrograms amounts of REEs and Y were also investigated. In the absence of reference materials with certified values of REEs and Y in zircon, ilmenite, rutile, and in columbite-tantalite, the accuracy of the proposed method was checked by analyzing a number of synthetic samples, Canadian Certified Reference Material Syenite Rock SY-2 sample solution (whose REEs and Y values are known) doped with milligram quantities of Zr, Ti, Nb, and Ta separately. In addition, an independent REE and Y separation was carried out by using the fluoride precipitation method. The accuracy achieved was very good (error within ±5%) for most of the elements. The RSD obtained by the present method varies from ~2% to 7% depending on the concentration of individual REEs used in this study. The method is accurate, precise, and suitable for the separation and ICP-AES determination of REEs and Y in different types of refractory minerals.

INTRODUCTION

The rare earth element (REE) geochemistry plays an important role in the interpretation of certain geological processes and REE distribution is influenced by magmatism (1) and sedimentation (2). Their distribution pattern is useful in understanding the petrogenesis of rock (3). The REE distribution patterns in zircon (4,5) qualitatively reflects the evolution and bulk chemical differences of their parent melt and can, therefore, be used for identification of the source. Identical REE patterns and close ratios of Zr/Hf, Th/U, and La/Th of zircon samples also prove conclusively that they belong to the same source. Association of REEs in rock-forming minerals such as amphiboles, biotite, garnets, feldspars, and magnetite, and their presence in banded iron oxide (6), is of great geochemical significance. It has been reported (7) that light and middle REEs plus yttrium have been systematically mobilized relative to the heavy REEs and other trace elements in the alteration pipes beneath the Canadian massive Cu-Zn sulphide deposits. Thus, an understanding of the distribution pattern of REEs is of great importance in geochemistry. However, the accurate determination of REEs in diversified geological materials, especially in refractory minerals, is a challenging task.

ICP-AES is a common geoanalytical technique and is widely used for the determination of refractory elements such as Ti, Zr, Hf, V, Nb, Ta,

Corresponding author.
e-mail: apremadas@yahoo.co.in

Sc, Y, REEs, and Th in rock samples due to the very high excitation temperature of the plasma. Moreover, this technique can achieve low detection limits and have a linear calibration range of 4–6 orders of magnitude, minimal chemical interference, in addition to being simple and fast in operation. However, this technique suffers from spectral and background continuum interferences due to the presence of major and minor matrix elements in the sample solution, especially if the concentration of analyte in the rock and mineral samples is very low. For complete decomposition of the refractory minerals, it needs fusion with either an alkaline (Na_2O_2 or Na_2CO_3) or an acidic flux (KHF_2 or $KHSO_4$) that adds large amounts of salt to the solution. The high salt load changes the excitation conditions of the plasma and also the emission spectra. Moreover, an element reported as non-interfering at lower levels falsifies the REE determination if present in high quantity. Therefore, a selective group separation and preconcentration of REEs is necessary before ICP-AES determination.

Cation exchange chromatography is widely used for the separation of REEs from geological samples and the method has undergone many modifications depending on the nature of the sample (8–13). It has been reported (14) that in the presence of very high amounts of iron and aluminum, and due to washing the column with ~1.7 N nitric acid for the elution of concomitant elements, there is a loss in the values of Sm, Eu, and Gd. It has also been observed that if the iron content in the sample is high (ilmenite or garnet), complete separation of iron from the REE fraction is difficult and requires prolonged washing. At higher concentrations, the high field strength elements such as Zr, Ti, Nb, and Ta hydrolyze in ~1 M hydrochloric acid or nitric acid solution, which is used for the

cation exchange separation. Moreover, no suitable ion exchange separation method of REEs is available for refractory minerals such as zircon, ilmenite, rutile, columbite-tantalite, garnet, and silliminite. It has been observed that in the presence of oxalic acid (0.2–0.3 M) elements such as Zr, Ti, Nb, and Ta could be stabilized in ~1 M hydrochloric acid. The moderately higher concentration of hydrochloric acid prevents the precipitation of rare earth oxalates.

This paper summarizes the separation, preconcentration, and ICP-AES determination of REEs in zircon, ilmenite, rutile, columbite-tantalite, garnet, and silliminite samples. Accuracy of the method was established by separating and determining microgram amounts of REEs and Y in synthetic mixtures, corresponding to a composition similar to these minerals. In natural samples, the accuracy was validated by carrying out an independent fluoride precipitation (15) separation of REEs and Y using calcium as the carrier and then removing it by solvent extraction (16). Accuracy was very good (error within ± 5%) for most of the elements, and the RSD obtained in the analysis of a natural zircon sample indicated a variation from 2–7% depending on the concentration of REEs and Y studied. The proposed method is simple, rapid, and very useful for the trace level separation and preconcentration of REEs from a matrix dominated by Zr, Ti, Nb, and Ta, followed by ICP-AES determination.

EXPERIMENTAL

Instrumentation

All ICP-AES measurements were performed using an Integra Model XM sequential spectrometer (GBC, Melbourne, Australia). The instrument is equipped with a rapid scanning monochromator (focal length 750 mm), ruled grating of 1800 grooves mm^{-1}, and Czerny-Turner

mounting system. All measurements were carried out under vacuum conditions. Details of the instrumental parameters and other operating conditions used are given in Table I.

All flame AAS measurements were made using a Spectra AA-20 atomic absorption spectrophotometer (Varian, Melbourne, Australia).

TABLE I
Operating Parameters
for ICP-AES

RF Generator	40.68 MHz (Free running)
Forward power	1200 W
Reflected power	<20 W
Gas flow	10.5 L min^{-1} coolant
	0.6 L min^{-1} sample
	0.3 L min^{-1} auxiliary
Monochromator	Modified Czerny-Turner
Focal length	750 mm
Light path medium	Vacuum
Diffraction grating	1800 grooves mm^{-1}
Ruled area	52 mm x 52 mm
Wavelength range	160-820 nm
Wavelength resetability	± 0.002 nm
Dispersion	0.74 nm mm^{-1} (first order)
Nebulizer	Concentric
Solution uptake	1.7 mL min^{-1}
Slits	20 μm entrance and exit
Detectors	Dual Photomultipliers
PMT voltage	675 V
Number of steps and time	40 steps, 0.2 sec
Observation height	11 mm above load coil

Reagents

All reagents and chemicals used were either AnalaR® (BDH, Pool, England) or GR quality. Specpure® rare earth oxide (Johnson Matthey, U.K.) was used for the preparation of standard solutions.

Preparation of Standards

A stock solution of 1000 μg mL^{-1} was prepared from rare earth oxides by dissolving in hydrochloric acid solution; the acidity was maintained at ~1 M HCl. A combined reference solution was prepared in 0.5 M HCl containing: 25 μg mL^{-1} each of Ce and Nd; 20 μg mL^{-1} each of La, Pr, and Sm; 10 μg mL^{-1} each of Gd, Tb, Dy, and Er; 5 μg mL^{-1} each of Ho, Tm, and Lu; 2 μg mL^{-1} each of Yb, Y, and Sc; and 4 μg mL^{-1} of Eu. For calibration, this stock solution was further diluted to 5, 10, 25, and 50 times, maintaining 0.5 M HCl.

Sample Decomposition

Zircon, Ilmenite, and Rutile Minerals

A sample amount of 0.500 g was placed into a 30-mL platinum crucible and mixed thoroughly with ~2.5 g of flux (a powdered mixture of KHF_2 and NaF in 3:1 ratio, hereafter referred to as flux). The contents were first melted on a low flame, then fused to red-hot condition for about five minutes to get a clear melt. The melt was cooled; during cooling, the melt was spread regularly over the walls of the crucible. Then ~6 mL (50%) sulphuric acid was added and slowly heated to achieve sulphur dioxide fumes. The contents were thoroughly stirred and mixed with a platinum rod and, when necessary, the lumps were crushed. The contents were then transferred into a beaker with water and 30 mL of ~0.8 M oxalic acid solution and 0.5 g boric acid were added. The contents (~150 mL) were boiled for about five minutes, and the acidity maintained around 1 N by addition of ~5 mL HCl for the ion exchange separation.

A duplicate of the above sample solution was prepared after fusion and subsequent sulphuric acid fuming. The contents were transferred into a beaker using hydrochloric acid (15 mL), then ~0.5 g boric acid was added and diluted to ~100 mL, and the contents boiled to get a clear solution. To the hot solution, excess dilute (1:1) ammonia was added until complete precipitation of zirconium hydroxide or titanium hydroxide had taken place, which also precipitates all REEs and Y (pH ~10). The beaker was kept on a steam bath for about 10 minutes. The precipitate was filtered through a Whatman No. 541 filter paper, the precipitate washed four times with 2% ammonia solution containing 2% NH_4Cl, and finally once with distilled water. The precipitate was transferred using a jet of water into the same beaker and the precipitate redissolved by boiling with a mixture of 10 mL HCl acid, 30 mL of 0.8 M oxalic acid and water, maintaining a total volume ~150 mL. The final acidity was kept around 1 N with HCl acid. Addition of a few drops of hydrogen peroxide is required for the dissolution of the hydroxide precipitates of rutile and ilmenite samples.

Columbite-Tantalite Minerals

Procedure A

A sample amount of 0.500 g to 1.000 g was placed into a silica crucible containing ~5 g $KHSO_4$ previously fused. The content was melted slowly on a low flame for ~10 minutes and then strongly fused for about 40 minutes with occasional swirling. The melt was cooled and transferred into a beaker containing 3 g oxalic acid and ~100 mL of water. The contents were boiled and taken out of the crucible. If any residue was left, it was filtered through a Whatman

No. 540 filter paper (12.5 cm). Then, the residue was ignited and fused with ~0.5 g flux, as described above, heated with 1 mL sulphuric acid (for the removal of fluoride), and the residue solution mixed with the original solution. Then ~5 mL of concentrated hydrochloric acid was added and the solution diluted with water to ~150-mL volume for cation exchange separation of REEs and Y.

Procedure B

A sample amount of 0.500 g to 1.000 g was placed into a platinum dish, 3 mL of 8 M H_2SO_4 and 10 mL each of concentrated hydrochloric acid and hydrofluoric acid were added, and the mixture covered with a Teflon® lid. The dish was placed on a boiling water bath and heated for two hours with occasional stirring; then the lid was removed and the volume reduced to ~5 mL. The process of evaporation was repeated by the addition of 10 mL each of hydrochloric and hydrofluoric acids, followed by evaporation with 10 mL hydrochloric acid alone to a volume ~5 mL. Then 45 mL of 0.4 M oxalic acid, 4 mL hydrochloric acid, and 3 g boric acid were added and warmed in a water bath for 10 minutes. The content was transferred into a glass beaker; if any residue was present, the residue was fused with 0.5 g of flux, as described above, and mixed with the original solution. The solution was diluted with water to ~150-mL volume and boiled for about 5 to 10 minutes to obtain a clear solution (add a few drops of hydrogen peroxide if necessary). The final volume was kept to ~150 mL for the cation exchange separation of REEs and Y.

Garnet and Silliminite Samples

A sample amount of 0.500 g to 1.000 g was placed into a platinum dish or Teflon beaker and treated three times with 10 mL HF (48%) and 10 mL HCl to incipient dryness with occasional stirring on a steam

bath or hot plate. Then 1 mL perchloric acid (~70%) and 10 mL HCl were added; again treated to incipient dryness, and finally to white fumes of perchloric acid on a hot plate. The content was digested with 15 mL of 4 M hydrochloric acid and transferred into a glass beaker using water. The residue was filtered through a Whatman No. 540 filter paper, ignited and fused with ~0.5 g flux (2 g flux is needed for 1 g of silliminite sample residue). While cooling, the melt was spread regularly over the walls of the crucible. Then, ~2 mL of 50% sulphuric acid was added (~6 mL for 1 g of silliminite) to the cooled melt and slowly heated on a low flame to disintegrate the fused melt. Then the crucible was covered with a lid and placed on a hot sand bath, then heated until the appearance of dense white fumes, which confirms the removal of fluoride ions. The residue was taken in water (~25 mL), the content mixed with the original solution, and about 1 g boric acid was added. The content was boiled and cooled. The solution was diluted to ~100-mL volume, maintaining ~1 N acidity for the cation exchange separation of REEs and Y.

The silliminite sample was hydrolyzed using ammonia solution (pH ~10) and the residue filtered and redissolved in hydrochloric acid, maintaining ~1 N (100 mL) for the cation exchange separation.

Cation Exchange Chromatography and ICP-AES Determination of REEs and Y

A chromatographic glass column, having an internal diameter of 2 cm, was fitted with a glass sinter disc and PTFE burette tap. The column was filled with Dowex cation exchange resin (SIGMA Chemical Company, USA) 50 x 8 (200–400 mesh size) up to a height of ~10 cm. The ion exchange column was cleaned with 400 mL of

6 M HCl and conditioned with 100 mL of 1 M hydrochloric acid. The sample solution (100–150 mL volume in ~1 N acidity) was passed through the column at the rate of ~1 mL min⁻¹. Afterwards, the interfering elements were eluted using ~150 mL of 1.5 N hydrochloric acid solution. The column was washed further with 15 mL of water and the REEs and Y eluted using 100 mL of 7 M nitric acid solution at the above rate. The REE fraction was collected in a beaker and ~2 mL of perchloric acid was added, then evaporated to dryness on a hot plate. The residue was treated with 4 M hydrochloric acid (~3 mL) by warming and then diluted with water to 25 mL in a volumetric flask (maintaining ~0.5 M HCl) for the ICP-AES determination of REEs and Y using the lines and the background correction points as shown in Table II.

TABLE II
Spectral Lines Used for Emission Measurements, Detection Limits, and the One-point Background Correction Applied

Element	λ (nm)	BGC (nm)		DL (µg L⁻¹)
		Left	Right	
La	333.749		0.02	2
Ce	418.660	0.02		27
Pr	422.293	0.02		43
Nd	430.358		0.02	30
Sm	442.434	0.02		17
Eu	381.967	0.02		0.3
Gd	342.247	0.02		2
Tb	350.917	0.02		10
Dy	353.170		0.02	6
Ho	345.600		0.02	5
Er	349.910		0.02	10
Tm	346.220		0.025	5
Yb	328.937		0.02	1
Lu	261.541		0.02	0.5
Y	371.170	0.02		1

Fluoride Precipitation Separation of REEs and Y

A 0.500-g sample was placed into a nickel crucible and mixed with ~7 g sodium peroxide, slowly sintered on a low flame burner, and the contents fused to molten red for about five minutes with occasional swirling. The contents of the nickel crucible were treated with water in a beaker, boiled, and the crucible removed. Then ~15 mL of hydrochloric acid was added and the solution diluted to ~300 mL, boiled and cooled. Dilute ammonia (1:1) solution was added to completely precipitate the hydroxide. The precipitate was filtered and washed with a solution containing 2% ammonium chloride in 5% ammonia solution. The precipitate was then transferred into the same beaker using a jet of water, and hydrochloric acid and the hydroxide precipitation was repeated once more. The precipitate was transferred into a platinum dish (80-mL capacity) using 10% hydrofluoric acid and 100 mg calcium was added as the carrier. The content was evaporated to a volume of ~15 mL in a water bath with 15 mL hydrofluoric acid (48%), and the evaporation continued as earlier. Then ~30 mL of water was added and the precipitate allowed to settle for about two hours. The precipitate was filtered through a Whatman No. 540 filter paper (12.5 cm) and the residue washed four times using 5% hydrofluoric acid. The residue along with the filter paper was transferred into the same platinum dish and slowly ignited to ~650ºC in a muffle furnace for about two hours. The dish was cooled, the residue dissolved in hydrochloric acid, and the solution transferred into a beaker. The content was evaporated to dryness and taken in 0.1 M hydrochloric acid (50 mL). The calcium, coprecipitated zirconium, titanium, niobium, and tantalum were removed by the solvent extraction procedure using

a mixture of mono-2-ethylhexyl hydrogen phosphate and bis-(2-ethylhexyl) hydrogen phosphate (16). The REE fraction was diluted to 25-mL volume for ICP-AES determination.

RESULTS AND DISCUSSION

The major problems in the ICP-AES determination of REEs and Y in refractory minerals are (a) preparation of a clear sample solution, (b) presence of very high quantity of salts in the sample solution derived from flux that is used for the fusion, and (c) spectral interference and background elevation caused in the presence of major and minor matrix elements. A simple repeated acid digestion using a mixture of hydrofluoric acid, hydrochloric acid, and perchloric acid does not completely decompose the zircon, ilmenite, rutile, columbite-tantalite, garnet, and silliminite samples. Therefore, the residue (undissolved material) after acid digestion treatment needs fusion with either an alkaline or acidic flux that increases the salt content of the solution. This makes the solution unsuitable for direct aspiration into the ICP-AES due to clogging in the concentric nebulizer. In addition, this will also elevate the background radiation, thus decreasing the detection limits. The easily ionizable elements (EIE) such as sodium, potassium, and calcium in higher amounts suppress the emission signal (17–19). Moreover, the high salt content hinders the preconcentration of REEs by the evaporation process. The spectral line-rich elements such as Zr, Ti, and Fe and to a lesser extent Nb and Ta, when present in very high quantity in sample solution, affect the emission signal of REEs. When some of the high field strength elements such as Zr, Ti, Nb and Ta are present at higher concentrations (0.5 to 2 mg mL^{-1}) in ~1 M hydrochloric acid medium (used for the ion exchange separation), they are hydrolyzed. Agents such

as oxalic, tartaric, or citric acid are needed to prevent this complexing. For this study, oxalic acid was selected since it offers better complexing ability towards zirconium and titanium.

Sample Decomposition

Zircon, Ilmenite, and Rutile Samples

These minerals were not easily decomposed by acid digestion; so direct fusion of these samples was necessary. A 0.500-g sample could easily be fused with ~2.5 g flux, and a 1-g sample required ~4 g flux. The entire fusion process takes about five minutes. The fluoride ion present in the flux was removed by heating with sulphuric acid. The use of a fluoride flux is also useful in removing the silica present in the sample, especially in the case of zircon where the fused mass was treated with sulphuric acid on a hot plate. During the disintegration process of the fused mass with sulphuric acid, it was necessary to crush the lumps with a platinum rod when a 1-g sample was taken for the analysis, so that the removal of fluoride content would be easier. However, for a 0.5-g sample, crushing the lumps was not required.

Columbite-Tantalite Minerals

These samples were decomposed by fusion with potassium bisulphate and usually gave a clear solution in ~0.25 M oxalic acid solution. If any unattacked residue remained, it was further fused with 0.5 g flux which was sufficient to decompose the residue (mainly cassiterite mineral). Since the total salt content is high, the solution was diluted to ~150-mL volume for the ion exchange separation. The acid digestion procedure using a mixture of hydrofluoric, hydrochloric, and sulphuric acid solution was also effective in decomposing the columbite-tantalite minerals. In this method, the salt content of the solution used for the ion exchange

separation was much less. By both decomposition procedures, 0.500–1.000 g samples could easily be taken up for the ion exchange separation of REEs and Y.

Garnet and Silliminite Sample

A repeated acid digestion of these samples using a mixture of hydrofluoric, hydrochloric, and perchloric acids, as described in the Experimental section, did not result in a clear solution. The small quantity of the residue that remains such as in the case of garnet (1 g) can easily be fused with 0.5 g flux, so that the overall salt content in the garnet sample solution (~100 mL) at the time of ion exchange separation was maintained around 0.5% or less. In case of the silliminite sample (~1 g), the acid digestion treatment dissolved only ~50% of the sample and the undissolved residue required around 2.0 g flux for fusion and the complete decomposition of the sample. The solution thus obtained by the above procedure was subjected to a hydroxide precipitation to remove the excess acid and the salt content before the ion exchange separation. Small quantities of fluoride ions, if any, remain even after the sulphuric acid fuming is complexed with a little boric acid. It was observed that excess fluoride ion in the solution affected the quantitative recovery of REEs.

Spectral Interference Study

Elements considered non-interfering in the ICP-AES determination of REEs and Y will begin to interfere at higher concentrations. Therefore, the effects of higher concentrations of Ti, Zr, Nb, Ta, and Fe were studied on the individual REEs and Y using the lines listed in Table II. The line selection was based mostly on work reported earlier (9–15) and the most frequently used sensitive and relatively interference-free lines were selected. The interferent element solution

having a concentration of 2 mg mL^{-1} of Nb, Ti, and Zr each and 0.5 mg mL^{-1} Ta was prepared in a mixture of 0.08 M oxalic acid and 0.5 M hydrochloric acid solution. The iron solution was prepared in 0.5 M hydrochloric acid medium. Each element was then scanned in a 0.1-nm window (41 steps, 0.2 seconds per step) and compared with the lowest calibration standard used. The presence of 2 mg mL^{-1} of Zr shows positive interference (due to spectral and background elevation) on all REEs and Y, except Sm, Gd, and Dy; 2 mg mL^{-1} of Ti shows interferences on La, Nd, Sm, Gd, Tb, Ho, Er, Tm, and Y; 2 mg mL^{-1} of niobium shows interferences on Sm, Eu, Gd, Er, Yb, and Y; and 0.5 mg mL^{-1} of tantalum shows interferences on Nd and Lu. This suggests that for an accurate determination of REEs and Y in samples like zircon, ilmenite, rutile, columbite-tantalite, garnet, and silli-minite it is necessary to separate these major matrix elements before ICP-AES determination of trace amounts of REEs and Y.

Cation Exchange Separation

The cation exchange chromatographic separation of REEs and Y in an igneous rock sample solution is normally carried out in ~1 M hydrochloric acid medium. However, elements such as Zr, Ti, Nb, and Ta get hydrolyzed at higher concentrations (>1 mg mL^{-1}), which are normally present in refractory minerals such as zircon, ilmenite, rutile, and columbite-tantalite. In this study, hydrolysis of these elements was prevented by the addition of oxalic acid (~0.25 M) which acts as a complexing agent. Among the various complexing agents studied like oxalic, tartaric, and citric acid it was noted that zircon samples could easily be dissolved in oxalic acid solution after the sample decomposition. The multiple elution peak observed for zirconium in an earlier work by

Crock et al. (20) was not found when oxalic acid was also added to the zirconium solution. In the presence of oxalic acid, zirconium forms an anionic zirconium oxalate complex, which was not adsorbed on the resin, and it could be easily washed out of the column. In order to study the recovery of REEs and Y in a zirconium-rich matrix, the ion exchange separation studies were carried out using a synthetic mixture containing (a) 500 mg Zr and microgram quantities of REEs and Y, (b) 1.000 g of SY-2 standard reference sample solution doped with

500 mg Zr, and (c) by carrying out an independent separation of REEs and Y like the fluoride precipitation separation using calcium as the carrier. A comparison of the results suggests very good recovery of all REEs and Y (see Table III). The presence of oxalic acid up to 0.25 M studied did not change the adsorption behavior of REEs and Y on the ion exchange column. However, it was observed that in the presence of very high salt and acid concentrations (in case of a 1-g sample taken for fusion), some heavy REEs, especially Yb and Lu, were partly lost (about 10–15%).

TABLE III
Ion Exchange Chromatographic and ICP-AES Determination of REEs and Y From Synthetic Zirconium-rich Matrix and Zircon Sample

Element	SYN-1		SYN-2		Zircon Proposed method		
	Spike	Found	RV^a	Found	A	B	C
La	50	51	74	76	68 ±2	69	70
Ce	100	96	175	168	164 ±3	168	165
Pr	45	44	18.8	19	11±0.7	12	11
Nd	85	84	73	78	54 ±3	56	54
Sm	40	42	16.1	14	9 ±0.5	10	9
Eu	7.0	6.8	2.42	2.40	2.0 ±0.02	2.0	2.2
Gd	50	52	17	16	26 ±1	27	25
Tb	20	21	2.5	3.0	5 ±0.3	5	5
Dy	20	20	18	19	64 ±2	66	68
Ho	10	11	3.8	4.2	18 ±1	18.5	19
Er	15	15	12.4	13	93 ±3	95	98
Tm	7.0	7.1	2.1	2.2	16.0±0.5	16.5	17.0
Yb	7.0	6.9	17	18	165±3	168	160
Lu	7.0	7.3	2.7	2.9	29.5±0.8	30.3	28.5
Y	50	49	128	122	607±20	610	600
Zr	500*	30	500*	40	50	60	40

All values are in microgram except those values with the (*) mark which are in milligram.

SYN-1= Synthetic mixture of 500 mg Zr and known microgram amounts of REEs and Y.

SYN-2= Synthetic mixture of 1.000 g syenite SY-2 reference standard solution spiked with 500 mg Zr.

^{a} RV = Recommended value (Govindaraju, Geostand. Newsl. 1994, Special Issue, Vol. XIII).

A= Direct ion exchange separation of zircon sample solution.

B= Ion exchange separation after the hydroxide precipitation of zircon sample solution.

C= The REE values obtained after the fluoride precipitation and solvent extraction separation of REEs and Y.

154

It was therefore necessary to minimize the salt content in the solution, and keep the total acidity at approximately 1 N at the time of ion exchange separation. One set of zircon samples, after fusion with the flux and subsequent sulphuric acid fuming, was also hydrolyzed (using ammonia solution) and the precipitate redissolved in a mixture of oxalic acid and hydrochloric acid solution for ion exchange separation to keep the salt content at a minimum. By carrying out the hydroxide precipitation, a 1-g zircon sample can be taken up for REE separation. The results obtained by the three different procedures are shown in Table III: (a) sample taken directly for the ion exchange separation, salt content ~1.5%, (b) after hydroxide precipi-

tation, that is negligible salt content, and (c) after fluoride precipitation separation using calcium as the carrier followed by removal of the calcium using the solvent extraction procedure. Complete recovery of REEs and Y was achieved in the synthetic mixture. In the case of the SY-2 sample solution, doped with 500 mg of zirconium, the REEs and Y values obtained agreed closely with the reported values. The total zirconium present in the REE fraction was less than 100 µg which is much below the interference level, whereas the co-adsorbed zirconium present in the fluoride precipitate of REEs using 100 mg calcium as the carrier was very high (1 mg Zr or higher). It was observed that with either the fluoride or the

oxalate precipitation separation of REEs and Y from the zircon sample solutions, the quantitative removal of zirconium is not possible. For comparison of REE values, the zirconium present in the REE precipitate, after fluoride precipitation, was removed by solvent extraction separation (16).

Table IV shows the recovery results of REEs and Y using the present method from a synthetic mixture of milligram amounts of Ti and microgram amounts of REEs and Y, and from SY-2 sample solution (1.000 g) doped with 500 mg Ti. Like zirconium, titanium also forms an anionic oxalate complex; therefore, it is easily washed out of the column, while the REEs and Y get adsorbed quantitatively on a resin around 1 N acid. The recovery

TABLE IV
**Ion Exchange Chromatographic Results of REEs and Y From Synthetic Titanium-rich Matrix
and From Ilmenite and Rutile Samples in the Presence of Oxalic Acid**

Element	SYN-1		SYN-2		Ilmenite			Rutile		
	Spike	Found	@RV	Found	A	B	C	A	B	C
La	50	49	75	77	38	40	39	53	58	54
Ce	100	102	175	166	75	77	73	105	110	106
Pr	45	48	18.8	20	3.8	4.0	3.8	10	11	11
Nd	85	81	73	80	20	22	18	42	43	45
Sm	40	38	16.1	18	–	–	–	6.8	7.0	6.8
Eu	7.0	7.1	2.42	2.40	0.60	0.61	0.61	0.60	0.61	0.62
Gd	50	49	17	18	2.5	2.5	2.3	6.0	5.6	6.1
Tb	20	21	2.5	3.0	0.5	0.5	0.5	0.6	0.6	0.7
Dy	20	20	18	18.4	1.4	1.5	1.7	5.0	5.0	4.9
Ho	10	10.5	3.8	4.2	<0.5	<0.5	<0.5	<0.5	<0.5	<0.5
Er	15	14.3	12.4	14	<0.5	<0.5	<0.5	5.0	5.0	5.2
Tm	7.0	6.7	2.1	2.4	<0.5	<0.5	<0.5	0.7	0.8	0.7
Yb	7.0	7.1	17	18	1.5	1.6	1.6	7.2	7.3	7.1
Lu	7.0	6.8	2.7	3.0	<0.5	<0.5	<0.5	1.0	1.1	1.0
Y	50	49	128	130	6.1	6.5	6.1	29	29	30
Ti	500*	20	500*	30	50	36	90	200	300	80

All values are in microgram except those values with the (*) mark which are in mg.
SYN-1 = Synthetic mixture of 500 mg Ti and microgram amounts of REE and Y.
SYN-2 = A 1.000 g syenite SY-2 reference standard solution doped with 500 mg Ti.
@RV= Recommended value (Govindaraju, Geostand. Newsl. 1994, Special issue, Vol. XIII).
A = Ilmenite or rutile (0.5 g) sample solution taken directly for ion exchange separation.
B= Ion exchange separation after the hydroxide precipitation of ilmenite and rutile sample solution.
C= Results obtained after fluoride and solvent extraction separation of REES using 100 mg Ca as carrier.

achieved was very good. Since the ilmenite sample contains very high amounts of iron, about 125 mL of 1.5 N hydrochloric acid solution was needed to wash the titanium and iron content of the ilmenite sample from the column. The Ti and Fe present in the REE fraction is also shown in Table IV. These small quantities of Ti and Fe do not cause any interference in the ICP-AES determination.

Table V shows the analytical results of REEs and Y from two synthetic mixtures of milligram amounts of Nb, Ta, Ti, Fe, and Mn and microgram amounts of REEs and Y using the proposed method. The REE and Y values obtained in the two columbite-tantalite reference materials IGS-33 and IGS-34 are also shown in Table V. For these reference samples, only the certified values of Nb, Ta, and Ti values are given (21). The recovery of REEs found by the proposed method is very good for both the synthetic sample as well as for IGS-33 and IGS-34 in comparison to the values reported by the acid hydrolysis method (22). Using the present method, a slightly higher value for cerium was noticed in the IGS-33 and IGS-34 samples. The major matrix elements other than Nb and Ta present in the REE fraction were much higher using the acid hydrolysis method than the proposed method (Table V). Though iron does not interfere in the ICP-AES determination of REEs up to a certain concentration ($\sim$0.5 mg mL^{-1}), it interferes at higher concentrations. The present method has the distinct advantage that it can be applied for the separation and preconcentration of the REE content in 1-g samples in a 25-mL volume, and the non-REEs present in the solution were much below the interference level.

TABLE V. Analytical Results of Ion Exchange Separation and ICP-AES Determination of REEs and Y From a Dominant Nb-Ta Matrix and Columbite-Tantalite Sample

| Element | Synthetic Sample | | | | Reference Standard Samples for Nb-Ta | | | | | |
| | SYN-1 | | SYN-2 | | IGS-33 | | | IGS-34 | | |
	Spike	Found	Spike	Found	IE	AH	F	IE	AH	F
La	100	103	50	51	130	134	140	137	120	130
Ce	120	122	60	59	510	426	530	305	268	330
Pr	95	95	50	48	39	42	35	45	39	40
Nd	120	120	60	61	175	166	165	176	178	177
Sm	95	96	50	48	56	61	54	173	219	170
Eu	19	19	10	10.2	1.9	1.6	1.81	4.0	3.5	4.2
Gd	50	48	25	26	88	85	84	287	307	295
Tb	50	47	25	24	24	25	20	70	73	60
Dy	50	50	25	24	185	195	190	275	293	290
Ho	25	26	10	9.3	36	44	35	30	28	26
Er	50	50	10	9.4	181	199	185	74	82	75
Tm	25	24	10	9.2	45	50	47	14	13	12
Yb	10	10	10	9.9	435	448	440	106	105	104
Lu	25	25	10	10.2	76	72	70	16	15	14
Y	10	10	10	9.8	970	983	900	900	891	830
Nb	238*	10	100*	10	20	20	800	20	20	400
Ta	20*	<20	200*	<20	<20	<20	500	<20	<20	1200
Fe	70*	85	70*	90	150	139.2	–	100	43.3*	–
Mn	10*	20	10*	25	40	1.69*	150	35	50.58*	800
Ti	10*	20	10*	25	20	1860	200	20	1260	150

All values are in microgram except those values with the (*) mark which are in milligram.

IE = Proposed ion exchange separation; AH = Acid hydrolysis method (Ref. 22); F = Fluoride precipitation separation method of REEs and Y (Ref. 22).

Sample	%Nb$_2$O$_5$	%Ta$_2$O$_5$	%TiO2	%FeO (T)	%MnO
IGS-33	68.79	5.46	1.80	17.80	2.12
IGS-34	27.45	49.83	1.20	5.80	8.80

Table VI shows the analytical results of REEs and Y in garnet and silliminite samples. The sample solution was passed through the column directly after adjusting the acidity to ~1 N. The aluminum present in the REE fraction (25 mL) was found to be 12–14 mg, whereas the iron and titanium content was much less. The interference study of aluminum on REEs shows that up to 1 mg mL^{-1} of aluminum there was no significant change in the emission signal of REEs.

Fluoride Precipitation and Solvent Extraction Separation of REEs and Y

Zr, Ti, Nb, Ta, Fe, Al, and Si form soluble fluorides in acidic medium, whereas REEs, Y, and Th form insoluble fluorides. Precipitation of REEs, Y, and Ca in hydrofluoric acid medium removes most of the Zr, Ti, Nb, Ta, Fe, and Al. However, in the presence of alkali metal ions, minor levels of Zr, Ti, Nb, and Ta also form insoluble double salts and accompany the REE fluoride precipitate. Therefore, it is necessary to remove most of the sodium derived from the flux. It was noticed that the presence of 1 mg mL^{-1} calcium in the solution causes 7 to 10% suppression in the emission signal of REEs and Y. For a 0.500-g sample diluted to 25-mL volume and using 100 mg calcium as the carrier, the concentration of calcium in the REE fraction would be ~4 mg mL^{-1} which affects the emission signal of all REEs and Y. Therefore, it is necessary to remove the calcium from the REE solution. The calcium was removed by solvent extraction separation and the amount of calcium found in the REE fraction was much below the interference level. In the absence of any suitable method reported in the literature, the fluoride precipitation method was used as a comparative method to check the accuracy of the proposed method.

Accuracy and Precision

In the absence of reference materials with certified values of REEs and Y in zircon, ilmenite, rutile, columbite, tantalite, garnet, and silliminite, the accuracy of the proposed separation method was checked by analyzing synthetic mixtures having a chemical composition similar to zircon, rutile, ilmenite, columbite, and tantalite, and containing known microgram amounts of REEs and Y and milligram amounts of Zr, Ti, Nb, and Ta separately. Accuracy of the method was also checked by spiking a 1.000-g SY-2 reference standard solution with 500 mg of Zr and Ti each, and 200 mg each of

TABLE VI
Analytical Results of REEs and Y From Garnet and Silliminite Samples

Element	Garnet				Silliminite			
	Fluoride Precipitation	Present method	(µg) REEs added*	(%) Recovery	Fluoride Precipitation	Present method	(µg) REEs added*	(%) Recovery
La	114	111	50	96	13	12	15	95
Ce	232	230	50	98	37	38	30	98
Pr	22	23	10	97	2.4	2.0	5	95
Nd	91	94	30	102	9	8	10	96
Sm	21	22	20	97	2.0	1.5	5	96
Eu	0.54	0.55	1.0	99	0.21	0.20	0.5	98
Gd	38	36	20	96	1.5	1.7	2	97
Tb	5	5	10	96	<1.0	<1.0	3	95
Dy	41	43	20	98	2.9	2.8	3.0	97
Ho	8	8	10	97	1.0	0.9	2.0	95
Er	25	27	20	96	3.7	3.5	3.0	96
Tm	2.8	3.0	3.0	101	0.4	0.4	5.0	99
Yb	24	26	10	100	6.5	6.4	5.0	99
Lu	3.1	3.1	2.0	98	0.4	0.4	2.0	98
Y	216	210	50	98	25	24	20	99

*Microgram amount of REEs and Y added to 1 g each of garnet and silliminite sample solution before cation exchange separation.

Composition	%SiO$_2$	%TiO$_2$	%Al$_2$O$_3$	%FeO	%MnO	%MgO	%CaO	%Na$_2$O	%K$_2$O
Garnet	37.0	1.20	21.0	31.0	0.30	7.30	1.0	0.01	<0.01
Silliminite	39.0	0.60	58.5	0.18	<0.01	0.06	0.39	0.04	0.01

niobium and tantalum, and then carrying out the proposed separation procedure. The recovery of REEs obtained by the proposed method of separation agreed well with the amount of REEs and Y taken, as well the values reported for the reference material SY-2. The results of the method also agreed closely with the fluoride precipitation method. In most of the cases, the error was within ±5%. The %RSD obtained for four independent separations and the determination REEs and Y on a zircon sample is shown in the Table III, which varies from 2-7% depending on the quantity of individual REEs. The method is simple and very good for the separation of REEs and Y from zircon, ilmenite, rutile, columbite-tantalite, garnet, and silliminite types of samples.

CONCLUSION

The cation exchange chromatographic method of REEs and Y in the presence of complexing agents such as oxalic acid is very useful for the separation of REEs and Y from the solution of refractory minerals such as zircon, ilmenite, rutile, and columbite-tantalite types of samples. No specific ion exchange separation procedure is available for these types of minerals.

A method was also developed for the separation of REEs and Y in garnet and silliminite. The sample decomposition procedure is very effective in bringing the refractory minerals completely into solution. Since the other matrix elements present in the REE fraction after the ion exchange separation is much less, 1-g samples can easily be concentrated in a 25-mL volume, which is ideal for the ICP-AES determination of REEs and Y.

REFERENCES

1. G.N. Hanson, Annu. Rev. Earth Planet. Sci. 8, 371 (1980).

2. S.M. McLennan, W.B.Nance, and S.R.Taylor, Geochim. Cosmochim. Acta 44, 1833 (1980).

3. P. Henderson, Rare earth element geochemistry, Elsevier, Amsterdam, Holland (1984).

4. A.V. Murali, R. Parthasarathy, T.M. Mahadevan, and M. Sankar Das, Geochim. Cosmochim. Acta 47, 2047 (1983).

5. T.S. Sunil Kumar, N. Krishna Rao, M.M. Palrecha, R. Parthasarathy, V.L. Shah, and K.K. Sinha, J. Geol. Soc. India 51, 761 (1998).

6. V.A. Makrygina and Ye.V. Smirnova, Geochem. International 22, 123 (1985).

7. I.H. Campbell, C.M. Lesher, P.Coad, J.M. Franklin, M.P. Gorton, and P.C. Thurston, Chem. Geol. 45, 181 (1984).

8. F.W.E. Strelow and P.F.S. Jackson, Anal. Chem. 46, 1481 (1974).

9. J.N. Walsh, F. Buckley, and J. Barker, Chem. Geol. 33, 141 (1981).

10. J.G.Crock and F.E. Lichte, Anal. Chem. 54,1329 (1982).

11. J.G. Crock, F.E. Lichte, G.O. Riddle, and C.L. Beach, Talanta 33, 601 (1986).

12. I.W. Croudace and S. Marshall, Geostand. Newsl. 15, 139 (1991).

13. M.C. Bruzzoniti, E. Mentai, and C. Sarzanin, Anal. Chim. Acta 352, 227 (1997).

14. K. Iwasaki and H. Haraguchi, Anal. Chim. Acta 208, 163 (1988).

15. I.B. Brenner, E.A. Jones, A.E. Watson, and T.W. Steele, Chem. Geol. 45, 135 (1984).

16. P.K. Srivastava and A. Premadas, J. Anal. At. Spectrom. 14,1087 (1999).

17. X. Romero, E. Poussel, and J.M. Mermet, Spectrochim. Acta 52B, 495 (1997).

18. I.B. Brenner, M. Zischka, B. Maichin, and G. Knapp, J. Anal. At. Spectrom. 13, 1257 (1998).

919. C. Dubuisson, E. Poussel, and J.M. Mermet, J.Anal. At. Spectrom. 13, 1265 (1998).

20. J.G. Crock, F.E. Lichte, and T.R. Wildeman, Chem. Geol. 45, 149 (1984).

21. R.B. Lister, Geostand. Newsl. 2, 157 (1978).

22. K. Satyanarayana, At. Spectrosc. 17, 69 1996).

SUBSCRIPTION INFORMATION

Atomic Spectroscopy
P.O. Box 3674
Barrington, IL 60011 USA
Fax: +1 (847) 304-6865

2003 Subscription Rates

- U.S. $60.00 includes third-class mail delivery worldwide; $20.00 extra for electronic file.
- U.S. $80.00 includes airmail delivery; $20 extra for electronic file.
- U.S. $60.00 for electronic file only.
- Payment by check (drawn on U.S. bank in U.S. funds) made out to: "*Atomic Spectroscopy*"

Electronic File

- For electronic file, send request via e-mail to: atsponline@yahoo.com

Back Issues/Claims

- Single back issues are available at $15.00 each.
- Subscriber claims for missing back issues will be honored at no charge within 90 days of issue mailing date.

Address Changes to:

Atomic Spectroscopy
P.O. Box 3674
Barrington, IL 60011 USA

Microfilm

Atomic Spectroscopy issues
are available from:
University Microfilms International
300 N. Zeeb Road
Ann Arbor, MI 48106 USA
Tel: (800) 521-0600 (within the U.S.)
  +1 (313) 761-4700 (internationally)

Guidelines for Authors

Atomic Spectroscopy serves as a medium for the dissemination of general information together with new applications and analytical data in atomic absorption spectrometry.

The pages of *Atomic Spectroscopy* are open to all workers in the field of atomic spectroscopy. There is no charge for publication of a manuscript.

The journal has around 3000 subscribers on a worldwide basis, and its success can be attributed to the excellent contributions of its authors as well as the technical guidance of its reviewers and the Technical Editors.

The original of the manuscript should be submitted to the editor by mail plus electronic file on disk or e-mail in the following manner:

1. Mail original of text, double-spaced, plus graphics in black/white.
2. Provide text and tables in .doc file and figures in doc or tif files.
3. Number the references in the order they are cited in the text.
4. Submit original drawings or glossy photographs and figure captions.
5. Consult a current copy of *Atomic Spectroscopy* for format.
6. Or e-mail text and tables in doc file and graphics in doc or tif files to the editor: anneliese.lust@perkinelmer.com or annelieselust@aol.com

All manuscripts are sent to two reviewers. If there is disagreement, a third reviewer is consulted.

Minor changes in style are made in-house and submitted to the author for approval.

A copyright transfer form is sent to the author for signature.

If a revision of the manuscript is required before publication can be considered, the paper is returned to the author(s) with the reviewers' comments.

In the interest of speed of publication, a pdf file of the type-set text is e-mailed to the corresponding author before publication for final approval.

Additional reprints can be purchased, but the request must be made at the time the manuscript is approved for publication.

Anneliese Lust
Editor, *Atomic Spectroscopy*
PerkinElmer
Life and Analytical Sciences
710 Bridgeport Avenue
Shelton, CT 06484-4794 USA

Axial Field™ Technology
Optimizes performance and speed in all matrices

Platinum Quick-Change Interface Cones
Easy maintenance, maximum uptime

PlasmaLok®
Easy optimization and extended cone life

Dynamic Bandpass Tuning
Efficiently screens out interferences while maximizing analyte transmission

AutoLens™
Optimizes voltage for each element

All-Quartz Sample Introduction
Minimizes contamination

SimulScan™
Simultaneous dual-stage detector with 9 orders of dynamic range

High-Speed Quadrupole
Fast transient signal analysis

AutoRes™
Custom resolution minimizes spectral interferences and improves detection limits

Dynamic Reaction Cell™ (DRC™) with Axial Field Technology provides superior interference reduction and performance for all applications.

Eliminates interferences COMPLETELY

When your applications extend beyond the capabilities of conventional ICP-MS, you need the power of the innovative ELAN® DRC II. The DRC II combines the power of patented Dynamic Reaction Cell (DRC) technology with performance-enhancing Axial Field Technology, providing uncompromised sensitivity and performance in all matrices for even the toughest applications. Unlike collision cell, high-resolution, or cold plasma systems, the DRC II completely eliminates polyatomic interferences providing ultratrace-level detection limits.

The DRC II uses chemical resolution to eliminate plasma-based polyatomic species before they reach the quadrupole mass spectrometer. This ion-molecule chemistry uses a gas to "chemically scrub" polyatomic or isobaric species from the ion beam before they enter the analyzer, resulting in improved detection limits for elements such as Fe, Ca, K, Mg, As, Se, Cr, and V.

Unlike more simplistic collision cells, patented DRC technology not only reduces the primary interference; it eliminates sequential side reactions that create new interferences. Unless kept in check by DRC technology, these uncontrolled reactions increase spectral complexity and create unexpected interferences.

PerkinElmer®
precisely.